MODELLING OF DOUBLY FED INDUCTION GENERATOR BASED WIND TURBINE

RAGHAV DHANUKA (109EE0268)

Department of Electrical Engineering
National Institute of Technology Rourkela

MODELLING OF DOUBLY FED INDUCTION GENERATOR BASED WIND TURBINE

A Thesis submitted in partial fulfillment of the requirements for the degree of

Bachelor of Technology in “Electrical Engineering”

By

Raghav Dhanuka

(109EE0268)

Under guidance of

Prof. P.K. Ray

Department of Electrical Engineering

National Institute of Technology, Rourkela

Rourkela-769008(ODISHA)

May, 2013

DEPARTMENT OF ELECTRICAL ENGINEERING

NATIONAL INSTITUTE OF TECHNOLOGY, ROURKELA

ODISHA, INDIA-769008

CERTIFICATE

This is to certify that the thesis entitled "Modelling of Doubly Fed Induction Generator Based Wind Turbine", submitted by **Raghav Dhanuka (Roll. No. 109EE0268)** in partial fulfillment of the requirements for the award of **Bachelor of Technology** in **Electrical Engineering** during session 2012-2013 at National Institute of Technology, Rourkela. A bona fide record of research work carried out by them under my supervision and guidance.

The candidates have fulfilled all the prescribed requirements.

The Thesis which is based on candidates' own work, have not submitted elsewhere for a degree/diploma.

In my opinion, the thesis is of standard required for the award of a bachelor of technology degree in Electrical Engineering.

Place: Rourkela

Dept. of Electrical Engineering
National institute of Technology
Rourkela-76900

Prof. P.K.Ray
Assistant Professor

ABSTRACT

There has been a constant rise in the use of renewable energy resources. Global wind energy capacity soared by a fifth to 238GW at the end of 2011. India being the 5th largest player globally, accounted for 16GW. Wind energy is an important form of renewable energy as there is no greenhousE gas emission compared to non-renewable fossil fuels. There has been a rising demand for wind energy ever since its first implementation.

This project work studies the power-speed characteristics and the torque-speed characteristics and the fundamentals of wind electrical systems along with the modeling of the various wind turbine features and simulation of the same using MATLAB-SIMULINK.

It deals with the vector control and modeling of the Doubly-Fed Induction Generator, which can be used to transmit power to the network through both the stator and the converters connected to the rotor. The turbine current, voltage, power and other characteristics are studied on variation of the grid parameters.

ACKNOWLEDGEMENT

I would like to articulate my sincere gratitude towards all those who have contributed their precious time and helped me along in my project work. Without them it would have been a tough job to complete and understand this project work.

I would especially like to thank Prof P.K.Ray, my Project Supervisor for his firm support and guidance and invaluable suggestions throughout the project work.

I express my greatest appreciation to Prof A.K.Panda Head of the Department, Electrical Engineering, and my Faculty Advisor Prof B.Chitti Babu and for their encouragement, comments and timely suggestions throughout the course of this project work. I express my indebtedness to all the faculty members and staff of the Department of Electrical Engineering, for their guidance and effort at appropriate times which has helped me a lot.

Raghav Dhanuka(109EE0268)

B.Tech Electrical Engineering

NIT Rourkela

CONTENTS

CHAPTER 2

DOUBLY FED INDUCTION GENERATOR

CHAPTER 3

MODELLING OF DFIG

CHAPTER 4

SYNCHRONIZED MODEL OF DFIG

CHAPTER 5

SIMULATION

CHAPTER 6

CONCLUSION AND FUTURE WORK

LIST OF FIGURES

NOMENCLATURE

d-q	Synchronously rotating reference frame direct and quadrature axes
d^s-q^s	Stationary reference frame direct and quadrature axes
$v_{ds}^s, v_{qs}^s, v_{dr}^s, v_{qr}^s$	Two axes stator voltages
$v_{ds}, v_{qs}, v_{dr}, v_{qr}$	Two axes rotor voltages
$i_{ds}^s, i_{qs}^s, i_{dr}^s, i_{qr}^s$	Two axes stator currents
$i_{ds}, i_{qs}, i_{dr}, i_{qr}$	Two axes rotor currents
$\psi_{ds}^s, \psi_{qs}^s, \psi_{dr}^s, \psi_{qr}^s$	Two axes stator flux linkages
$\psi_{ds}, \psi_{qs}, \psi_{dr}, \psi_{qr}$	Two axes rotor flux linkages
θ_e	Angle of synchronously rotating frame
θ	Angle of stationary reference frame
R_s	Stator resistance
R_r	Rotor resistance
ω_e	Synchronous speed
ω_r	Rotor electrical speed
ω_m	Rotor mechanical speed
ω_b	Angular frequency
f	Supply frequency
L_{ls}	Stator leakage inductance
L_{lr}	Rotor leakage inductance
L_s	Stator inductance

L_r	Rotor inductance
L_m	Magnetizing inductance
P	Number of poles
T_e	Electromagnetic Torque
T_L	Load Torque
J	Rotor Inertia
B	Damping Constant
$u_{d1}, u_{q1}, u_{d2}, u_{q2}$	2-axis voltages
$i_{d1}, i_{q1}, i_{d2}, i_{q2}$	2-axis currents
$\psi_{d1}, \psi_{q1}, \psi_{d2}, \psi_{q2}$	2-axis flux linkages
L_1, L_2	Machine inductances
L_m	Mutual inductances
r_1, r_2	Machine resistances
ω_1, ω_2	Stator and rotor frequency
ω_r	Rotor speed
U_1, U_2	RMS voltages
I_1, I_2	RMS currents
P_1, P_2	Active Power
Q_1, Q_2	Reactive Power
δ	Power Angle
ϕ	Power factor angle
σ	Leakage factor

E'_q	Internal transient EMF
J	Moment of inertia
ψ_1, ψ_2	Flux linkage vectors
X'_1	Stator transient reactance
X'_1	Stator reactance
X_m	Mutual reactance
T_{em}	Electromagnetic Torque
T_m	Input torque
s	Rotor slip
p	Differential operator

Sub scripts

d, q	d-q(synchronous axes)
1,2	stator, rotor

CHAPTER 1

Introduction

CHAPTER I: INTRODUCTION

1.1 Motivation

There is a general acceptance that the burning of fossil fuels is having a significant influence on the global climate. Effective changes in climate change will require deep reductions in greenhouse gas emissions. The electricity system is viewed as being much easier to transfer to low-carbon energy sources than more challenging sectors of the economy such as surface and air transport and domestic heating. Hence the use of cost-effective and reliable low-carbon electricity generation sources, in addition to demand-side measures is becoming an important objective of energy policy in most countries. Over the past few years, wind energy has accounted for the fastest rate of growth of any form of electricity generation with its development stimulated by concerns over climate change, energy diversity and security of supply by national policy makers. The maximum extractable energy from the 0-100 meters layer of atmosphere has been estimated to be around 10^{12} kWh per annum, which is of the same order as hydro-electric potential.

Advantages of using wind energy:

1 Since it is powered by wind, it is a clean fuel source and doesn't have harmful effects on the environment unlike fossil fuels which rely on combustion of coal, natural gas etc. It also doesn't produce emissions such as greenhouse gases and doesn't cause acid rain.

2. Its available in abundance and its sustainable, just needs to be harnessed.

3. It relies on the renewable power of wind which is in fact a form of solar energy. Winds are caused by non-uniform heating of atmosphere by sun, the rotation of earth and earth's surface irregularities.

4. Its low-priced costing just between 4-6cents per kWh and can be built on farms or ranches benefiting the rural economy where the best wind sites are located.

1.2 Relevant Terms:

Power Contained in Wind: This is the same as the kinetic energy of the flowing air mass per unit time given by

$$P_0 = \frac{1}{2}(\rho \mathrm{A} \mathrm{V}_\infty)(\mathrm{V}_\infty{}^2) .$$

$$\Rightarrow P_0 = \frac{1}{2}\rho A V_\infty{}^3 \tag{1.1}$$

Betz limit: It gives the maximum energy which can be extracted from the wind and is given by

$$P_{\max} = \frac{16}{27} P_0 = \frac{8}{27}\rho A V_\infty{}^3 \tag{1.2}$$

Tip Speed Ratio: The tip speed ratio (TSR) of a wind turbine is defined as

$$\lambda = \frac{2\pi R N}{V_\infty} \bullet \tag{1.3}$$

1.3 Types of Wind Turbines:

1.3.1 Horizontal Axis Wind Turbines (HAWT):

A horizontal axis wind turbine has its blades rotating on an axis which is parallel to the ground. It is the most common type of wind turbine.

Advantages of HAWT:

Variable blade pitches providing the suitable angle of attack and greater control along with better efficiency. It's located on a taller tower therefore subjected to greater wind speeds. Usually a 10m increase in the height of tower provides 20% increase in wind speed. Since the blades move at an angle complimentary to the wind speed therefore the drag force is greatly reduced which increases the power output.

Disadvantages of HAWT:

Greater construction costs due to larger structure. Also the transportation costs increase significantly. Production of noise affects radar operations. Greater wind speeds and turbulence may lead to structural failures. Additional Yaw Control mechanism is required.

Horizontal axis wind turbines can be further classified into:

A) "Dutch-type" grain-grinding windmills:

B) Multi-blade Water Pumping windmills:

C) High Speed Propeller-type Wind Turbine

1.3.2. Vertical Axis Wind Turbines (VAWT):

A VAWT has its blades rotating on an axis perpendicular to the ground. It's not used widely for commercial purposes compared to HAWT.

Advantages of VAWT:

Mounted close to ground so taller structures not required. It has lesser costs and easier maintenance, lower startup speed and lower noise. Yaw control mechanism is not required.

Disadvantages of VAWT:

It has lower efficiency due to additional drag force, due to lower heights they can't capture greater wind speeds at higher altitudes, generally they need additional startup mechanisms as they have zero starting torque.

Types of VAWT:

A) Savonious Wind Turbines:

B.) Darrius Wind Turbine

1.4 CONTROL METHODS FOR WIND TURBINE

1.4.1. Terms related to Aero-foil Dynamics:

- Pitch Angle - Angle between the aero-foil chord and plane of rotation.
- Angle of inclination- Angle between relative velocity vector and plane of rotation.
- Angle of incidence (attack) - Angle between relative velocity and the chord line.
- Drag Force- Force along the direction of relative wind velocity.
- Lift Force- Force normal to the relative wind velocity.
- Thrust Force- Component of total force along wind velocity.
- Torque Force- Component of total force along aerofoil velocity.

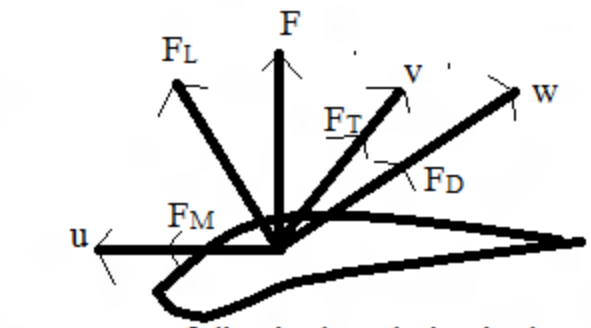

u,v,w- aerofoil velocity,wind velocity, relative wind velocity.
F_L,F_D- Lift force, Drag force
F_T,F_M- Thrust force, Torque force

Fig 1.1: Aerofoil Dynamics

1.4.2 Types of control in wind turbine:

a) Pitch Control: Angle between rotation plane and turbine blade is varied. It depends on the wind speed, rotor speed and power output. Blades are turned out when the power is too high, they are turned in when the power is too low. It's a relatively faster method and can be used to limit the rotor speed by regulating input aerodynamic flow of power, it has good power control, an assisted startup and an emergency stop. Unlike stall control it needn't be shut down beyond a certain speed. Efficiency decreases at high wind speeds as the pitch angle is increased to drop some power.

b) Stall Control: It is simple, cheap, and robust and its inherent aerodynamic properties of the rotor blade help in determining the output power. The aerodynamically designed blades help the rotor in stalling (losing power). It is used in constant speed wind turbines. As the wind speed increases the lift force decreases and drag force increases. It is noisy, sensitive to particles on the

blade and initial blade angle and has lower efficiency compared to pitch control, even at rated speeds.

c) Active Stall: Combination of pitch control and passive stall control. The blades are pitched similar to pitch controlled turbine at low and medium speeds. Unlike a passive stall there is no drop in power at higher speeds as the blades are rotated by a few degrees in the opposite direction compared to that in pitch controlled. Smoother limited power without fluctuation and can compensate any variation in air density.

1.5. Overview of proposed work done:

References [1] and [2] give us an overview of the principles and characteristics of the doubly fed induction generator. References [3] and [4] give us an idea of the basic working of wind turbines and all the theory related to types of wind turbines, power and torque characteristics and the theory of induction generators needed for the modelling. Reference [5] is helpful for finding out the aerodynamics behind the propeller type horizontal wind turbines. References [7] and [8] summarize the dynamic modelling of the turbine under various fluctuations whereas Reference [6] is more helpful in the control of the turbine. Reference [9] and [10] is the previous work done related to this field and give us the complete overview of this project work.

1.6. Thesis Objectives:

The following objectives are to be attained hopefully at the end of this project work:

1) Theory of wind turbine, various types of wind turbines, and the functioning mechanism of the different parts of the turbine along with the power and torque speed characteristics curve

2) Various control strategies pertaining to the wind turbine.

3) The operating principles and circuit model of the DFIG along with the power and torque relations and the equations and simulation for rotor injected emf.

4) Vector control using d-q transformation and modelling of various parts of the turbine.

5) Study of a DFIG wind farm with fluctuations in voltage, wind, reactive power demand.

1.7. Organization of Thesis:

The thesis is divided into five parts where each chapter focuses on an independent theory required to proceed further.

Chapter1 deals with the fundamentals of the wind turbine and the different types of turbines present and shows the advantages of the using wind turbine for energy generation purpose. It also compares the vertical and horizontal types of wind turbines along with the aerodynamics present. Lastly it covers the different control strategies for both fixed and constant types of wind turbines.

Chapter2 deals with the doubly fed induction generator in detail and the basics of DFIG and operation principles. It then focuses on finding out the equivalent circuit model for the same and the power and torque relations leading to four modes of operations. The equations for rotor injection are then found out which are used for simulation of the torque speed characteristics for rotor injection.

Chapter3 deals with the vector control theory and the d-q transformation to convert the three phase parameters into two phase so that further modelling may be achieved. The equivalent d-q

circuit in the synchronous frame of reference is then found out and expressions for stator, rotor and flux linkage are also found out.

Chapter4 describes the synchronized model of the DFIG and the modelling of the stator, rotor and the active and reactive power equations for the stator and rotor side.

Chapter5 is on Matlab simulation of various curves. It includes the power coefficient and tip-speed characteristics for different blade angles for the propeller type wind turbine, power and rotor speed characteristics curve for various wind speeds, torque speed characteristics for rotor injected e.m.f., and the study of an average model of the wind farm and simulation of the same under various voltage, wind and reactive power fluctuations.

CHAPTER 2

Doubly Fed Induction Generator

CHAPTER II: DOUBLY FED INDUCTION GENERATOR

2.1. Introduction

In a Fixed Speed Wind Turbine, the stator is connected to the grid directly. However, in a variable speed turbine the turbine control is done through a power electronic converter. Reasons for using a variable speed turbine include higher yield in energy, pitch control, lesser mechanical loads, control of active and reactive power, noise reduction, and lesser variation in power output.

The DFIG is one of the machines which employ the principle of variable speed.

Unlike other generators, the DFIG delivers power to the grid through both stator and rotor terminals. The stator is directly connected to the grid while the rotor is connected to the grid via power electronic converters.

Wind turbines usually employ DFIG having Wound Rotor Induction Generator.

The power electronic converter is an AC/DC/AC IGBT based PWM converter. The stator winding is connected directly to the grid (50Hz) while rotor is fed via the AC/DC/AC converter at a variable frequency. The optimum speed of turbine for which maximum energy (mechanical) can be produced for a given speed of wind is proportional to the wind speed.

2.1.1. Advantages of DFIG:

1. The ability of the power electronic converters to control the reactive power (absorption or generation), without employing capacitor banks unlike squirrel cage induction generator.
2. The converters only have to handle a small amount (20-30%) of the total power leading to lower losses in the electronic circuit.

3. This type of arrangement allows for maximum energy extraction from the energy in the wind by optimizing the turbine for lower speeds of wind while during higher wind speeds the mechanical stresses are reduced.
4. Improved Efficiency
5. Power Factor control

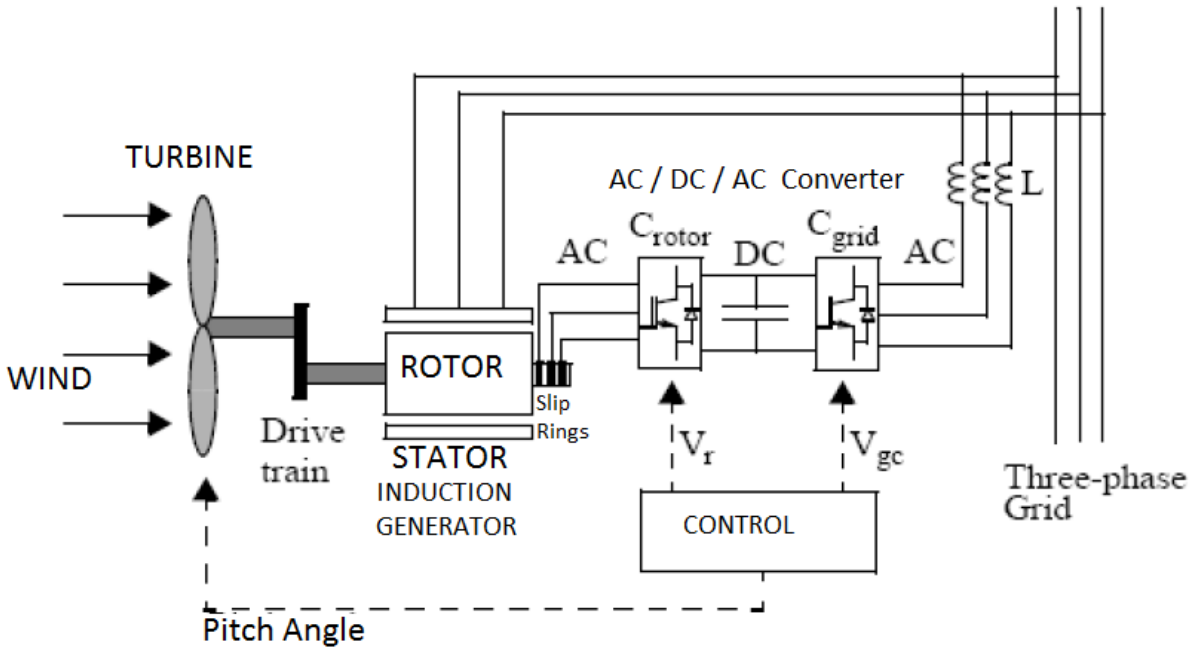

Fig 2.1: DFIG system with converters, turbine and grid.

2.1.2. Functioning mechanism of the basic blocks:

The basic diagram of a DFIG is shown above. The Stator is connected to the mains directly, as shown. The Rotor is fed through the power electronics converters present, via the slip rings. This permits the DFIG operation at various speeds depending on the changing speeds of wind.

The AC/DC/AC converter is usually a PWM (Pulse Width Modulation) converter. It employs sinusoidal PWM technique for reduction of harmonics present in the system. It has two components, C_{rotor} and C_{grid}. They are voltage source converters which employ forced commutation (IGBT) devices to generate AC voltage from a DC source.

The basic requirement is that of including a frequency conversion device which can act as a medium for connection between the varying frequencies of the generator the fixed frequency of the grid.

A capacitor connection is made on the DC side. It works as a DC source of voltage. It also decreases the voltage fluctuations (ripple) in the DC-link voltage. The DC capacitor links the rotor side converter (C_{rotor}) and the grid side converter (C_{grid}), permitting the power storage from the generator for generating purpose. If complete controlling of the grid current is required then the level of the DC-link voltage should be increased until it is greater than the line-to-line voltage amplitude.

The slip rings connection of the generator is made on the rotor side converter that has a DC link with the converter on the grid side. This type of connection is called back -to-back configuration. Power flow through the slip rings can take place in both the directions. In first case, power flows from the mains to the rotor and in the second case the power transfer takes place from the rotor to the supply. Therefor speed control of the machine can take place from either rotor side converter or grid side converter. The power in wind is extracted by the turbine and then it is converted into electrical power in the Induction Generator and sent to the grid via stator and rotor terminals. The command for the pitch angle and voltage is sent by the control system to the rotor side converter (C_{rotor}) and grid side converter (C_{grid}) for controlling the wind turbine power, the DC link voltage and reactive power at the grid windings.

C_{rotor} controls the torque and speed of the generator. It also controls the power factor at the stator terminals whereas C_{grid} maintains the DC link voltage constant. The back to back converter arrangement sets the stage for the conversion of the varying generator frequency and voltage output to constant voltage and frequency, at par with the grid.

The Gearbox is used to ensure that the maximum rotor speed occurs at the rated generator speed.

2.2. Operating Principle:

Once the speed of the rotor exceeds that of the rotating magnetic field of the stator (synchronous speed), a current is induced in rotor windings. With increase in the rotor speed, power is transferred to the stator via electromagnetic mechanism, and is then supplied to the electric grid through the stator terminals. The induction generator speed varies with the load torque. The difference between the rotational speed of the rotor and the synchronous speed of the stator flux is measured in percentage and is called the slip of the machine. The rotor and grid side converters allow the slip control of the DFIG. The slip power is regained for higher rotational speeds and sent to the grid, accounting for a more efficient operation. For reduced speed of the rotor, the ratings of the converters are similarly rated with lower ratings in comparison with the generator. This accounts for reduction of the system costs and losses.

For generation of power the mechanical torque being applied at the rotor is positive and also since the speed of the flux in the stator-rotor air gap is positive and constant(for constant frequency of grid), therefore slip sign accounts for the sign of power output from the rotor terminals. C_{rotor} and C_{grid} help in the production or absorption of the reactive power; they are used

for the control of reactive power or the voltage at the grid terminals. Pitch control can be employed for limiting the power output of the generator at higher speeds of wind.

$$P_m = T_m * \omega_r \tag{2.1}$$

$$P_s = T_{em} * \omega_s \tag{2.2}$$

Neglecting losses in generation,

$$J\frac{dw_r}{dt} = T_m - T_{em} \tag{2.3}$$

At steady state, for constant speed generation,

$$T_m = T_{em} \tag{2.4}$$

$$P_m = P_s + P_r \tag{2.5}$$

Therefore,

$$P_r = P_m - P_s = T_m\omega_r - T_{em}\omega_s$$
$$\Rightarrow P_r = T_{em}(\omega_r - \omega_s) = \frac{T_{em}}{\omega_s}\omega_s(\omega_r - \omega_s)$$
$$\Rightarrow P_r = (\omega_s T_{em})\left(\frac{\omega_r - \omega_s}{\omega_s}\right)$$

$$\therefore P_r = -sP_s \tag{2.6}$$

Where, slip, $s = \dfrac{\omega_s - \omega_r}{\omega_r}$

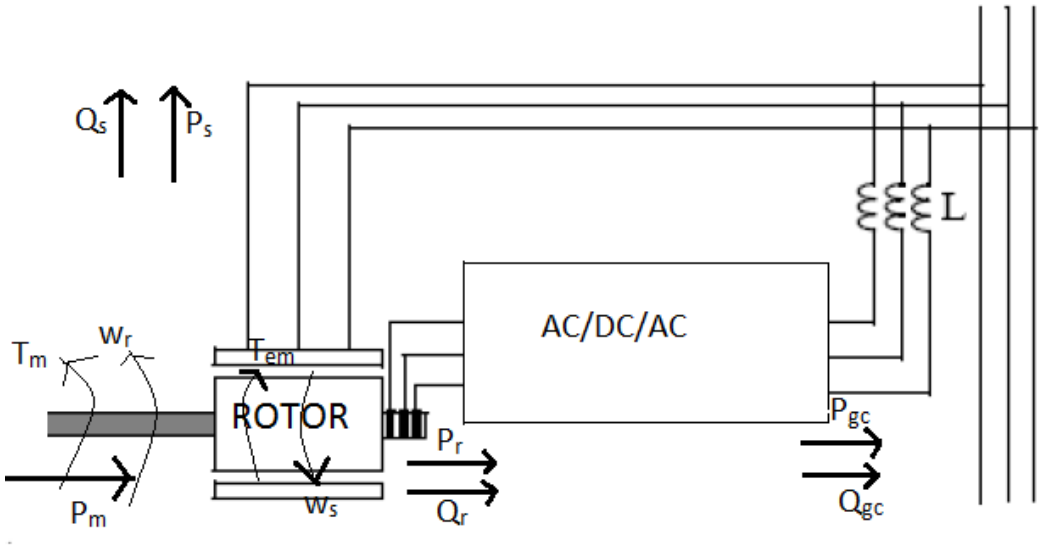

Fig 2.2: Power Flow in DFIG

Usually the magnitude of slip s is below 1, so P_r is small compared to P_s, the mechanical torque T_m is positive (during generation), synchronous speed ω_s is positive and fixed (for constant frequency at grid), and therefore the sign of P_r depends on the sign of slip. It's positive when slip is negative (for rotational speeds above the synchronous speed) and negative when slip is positive (for rotational speeds below the synchronous speed).

During super synchronous mode, P_r is sent to the DC link capacitor which raises the DC voltage. During sub synchronous mode, P_r is extracted from the capacitor lowering the DC voltage. The grid converter then extracts or delivers the grid power to keep the dc voltage fixed. During steady state, P_{gc} is equal to P_r, also the turbine speed can be found out from P_r extracted by or fed to C_{rotor}. The phase sequence of AC voltage produced by C_{rotor} depends on rotor speed and is positive when rotor speed is less than synchronous speed and negative when rotor speed exceeds the synchronous speed. The magnitude of the frequency of this AC voltage is slip times the frequency of the grid.

2.3. Equivalent Circuit Model:

Stator Circuit:

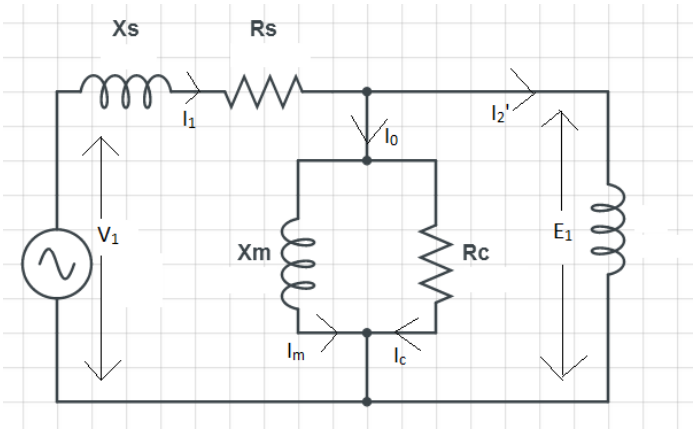

Fig 2.3: Stator Circuit

$$V_1 = E_1 + I_1(R_s + jX_s) \tag{2.7}$$

$$E_1 = 4.44 f k_{w1} T_1 \phi_m \tag{2.8}$$

Rotor Circuit:

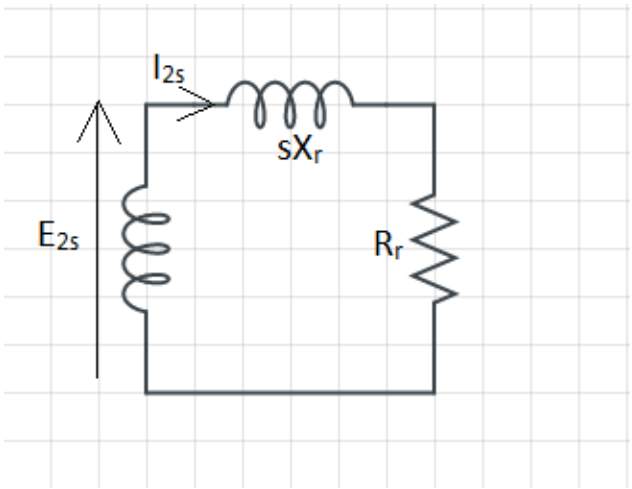

Fig 2.4: Rotor Circuit at slip frequency

$$E_{2s} = 4.44 s f k_{w2} T_2 \phi_m = \frac{4.44}{m} s f k_{w1} T_1 \phi_m$$

$$=> E_{2s} = \frac{sE_1}{m} \tag{2.9}$$

Where, $m = \frac{k_{w1}T_1}{k_{w2}T_2}$

$$I_{2s} = \frac{E_{2s}}{R_r + jsX_r} = \frac{sE_1}{m(R_r + jsX_r)} \tag{2.10}$$

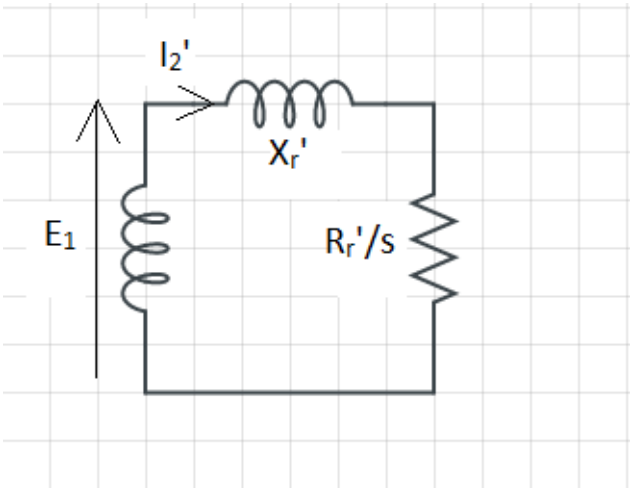

Fig 2.5: Rotor Circuit at Stator Frequency

$$I_2' = \frac{I_2}{m}$$

$$I_2' = \frac{E_1}{\frac{R_r'}{s} + jX_r'} \tag{2.11}$$

Where,

$$R_r' = m^2 R_r$$
$$X_r' = m^2 X_r$$

Note that the phase angle remains the same for both the rotor circuits, i.e.:

At slip frequency, $\phi_2 = \tan^{-1}\frac{sX_r}{R_r}$

At line frequency, $\phi_2 = \tan^{-1}\dfrac{X_r}{\dfrac{R_r'}{s}} = \tan^{-1}\dfrac{m^2 X_r}{\dfrac{m^2 R_r}{s}} = \tan^{-1}\dfrac{sX_r}{R_r}$

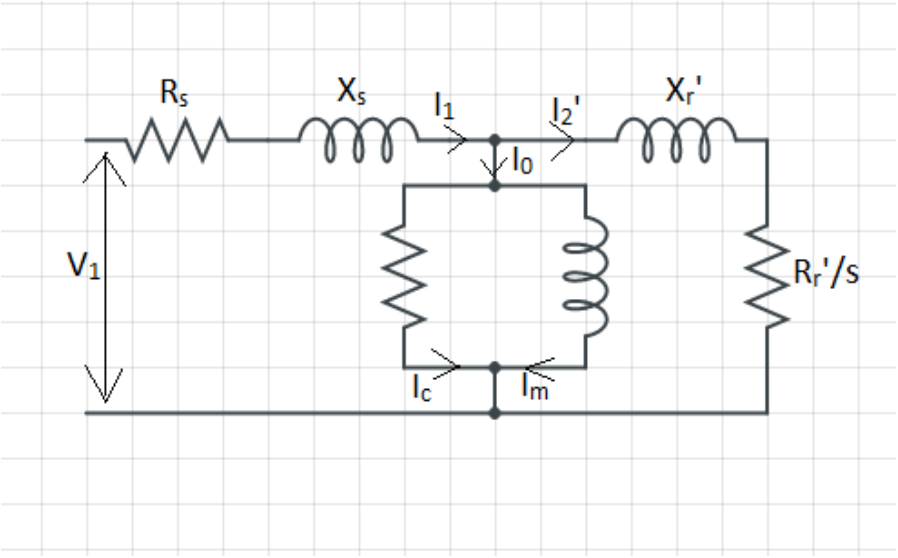

Fig 2.6: Complete Equivalent Circuit (at Stator Frequency)

2.4. Power and Torque Relations:

2.4.1. Power:

1. Power input to the rotor (Power transmitted across the air gap):

$$P_{ri} = 3E_1 I_2' \cos\phi_2$$

$$\Rightarrow P_{ri} = \frac{3I_2'^2 R_r'}{s} \qquad (2.12)$$

2. Power lost in the rotor (Rotor Cu Loss)

$$P_{rl} = 3I_{2s}^2 R_r = 3(mI_2')^2\left(\frac{R_r'}{m^2}\right) = 3I_2'^2 R_r'$$

$$\Rightarrow P_{rl} = sP_{ri} \qquad (2.13)$$

3. Mechanical Power (Rotor Power Output)

$$P_m = P_{ro} = P_{ri} - P_{rl}$$

$$\Rightarrow P_m = 3I'_2 R'_r \left(\frac{1-s}{s}\right)$$

$$\therefore P_m = (1-s)P_{ri} \tag{2.14}$$

2.4.2. Torque:

$$T_{em} = \frac{P_m}{\omega_r} = 3I'^2_2 R'_r \left(\frac{1-s}{s}\right) * \frac{1}{\omega_r}$$

$$\Rightarrow T_{em} = \frac{3I'^2_2 R'_r}{s} * \frac{1}{\omega_s} = \frac{P_{ri}}{\omega_s} \tag{2.15}$$

Torque-Speed Characteristics:

$$T_{em} = \frac{3}{\omega_s} * \frac{k^2 V_1^2 (R'_r + R'_x)/s}{[R_1 + (R'_r + R'_x)/s]^2 + [X_1 + X'_r]^2} \tag{2.16}$$

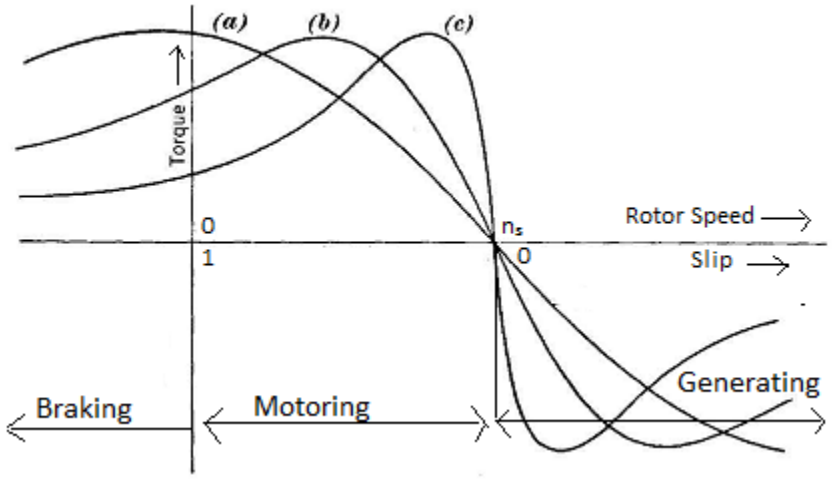

Fig 2.7: Torque-Speed Characteristics Curve for varying external resistance

The torque-speed characteristics curve is show above.

2.5. DFIG- Rotor Injected EMF:

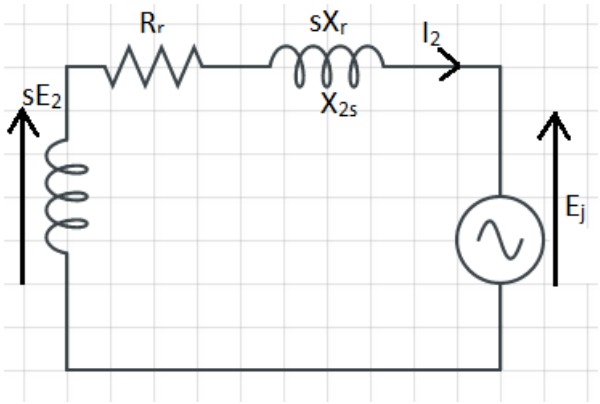

Fig 2.8: Rotor Injection

In a DFIG, unlike an induction generator, there is a rotor injected e.m.f. present. For the same, the circuit equations are as follows:

$$\begin{aligned} &sE_2 = I_2 z_{2s} + E_j \\ &\Rightarrow sE_2 \cos\phi_2 = E_j \cos(\phi_2 + \beta) + I_2 R_r \end{aligned} \tag{2.17}$$

Where, ϕ_2 - angle between sE_2 and I_2

β - angle between E_2 and E_j

$$\Rightarrow sE_2 I_2 \cos\phi_2 = I_2^2 R_r + E_j I_2 \cos(\phi_2 + \beta)$$

Referring to the stator,

$$sE_1 I_2' \cos\phi_2 = I_2'^2 R_r' + E_j' I_2' \cos(\phi_2 + \beta)$$

$$\therefore E_1 I_2' \cos\phi_2 = P_{ri} = P_{ag} \tag{2.18}$$

Also,

$$\begin{aligned} &\because I_2'^2 R_r' = P_{rl} \\ &E_j' I_2' \cos(\phi_2 + \beta) = P_2 \end{aligned} \tag{2.19}$$

$$\therefore sP_{ag} = P_{rl} + P_2 \tag{2.20}$$

Also, $(1-s)P_{ag} = P_m$

$$\Rightarrow P_{ag} = P_{rl} + P_2 + P_m \tag{2.21}$$

Thus, 4 modes of operation can be observed as shown in the following table:

Table 2.1: Modes of operation of the DFIG

	Mode-I Sub-synchronous Motoring	**Mode-II Super-synchronous Motoring**	**Mode III Sub-synchronous Generating**	**Mode-IV Super-synchronous Generating**
Slip(s)	s<1	s<0	0<s<1	-1<s<0
P_m	P_m>0	P_m>0	P_m<0	P_m<0
P_{ag}	P_{ag}>0; P_{ag}>P_m	P_{ag}>0; P_{ag}<P_m	P_{ag}<0;| P_{ag}|>|P_m|	P_{ag}<0;| P_{ag}|<|P_m|
P_{rl}+P_2:(sP_{ag})	sP_{ag}>0	sP_{ag}<0	sP_{ag}<0	sP_{ag}>0
P_2	P_2>0	P_2<0	P_2<0	P_2>0

$$P_m = (1-s)P_{ag}$$

$$\Rightarrow P_m = 3\frac{1-s}{s} I_2'^2 R_r' + 3\frac{1-s}{s} E_j' I_2' \cos(\phi_2 + \beta)$$

Let $m_1 = \frac{kw_1T_1}{kw_2T_2} = 1$

$$\Rightarrow P_m = 3\frac{1-s}{s}\left[I_2^2 R_r + E_j I_2 \cos(\phi_2 + \beta)\right]$$

$$\Rightarrow T_{em} = \frac{P_m}{\omega_r} = \frac{P_m}{(1-s)\omega_s} = \frac{3}{\omega_s s}\left[I_2^2 R_r + |E_j||I_2|\cos(\phi_2 + \beta)\right] \tag{2.22}$$

Where, I_2 can be found from the circuit shown below

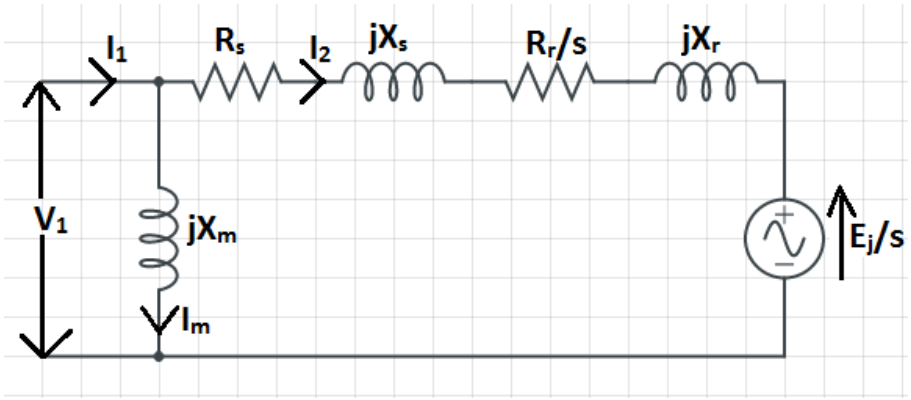

Fig 2.9: Simplified Equivalent circuit to find I_2

From the above figure,

$$I_2 = \frac{V_1 - E_j/s}{(R_s + R_r/s) + j(X_s + X_r)}$$

$$\Rightarrow |I_2| = \frac{|sV_1 - E_j|}{\sqrt{(sR_s + R_r)^2 + (X_s + X_r)^2}} \qquad (2.23)$$

2.6. Conclusion

The basic functioning mechanism of the DFIG was studied in detail and the advantages of the DFIG are visible and therefore its employed in the wind turbine generation. The operating principle for the same was studied in depth and the equivalent circuit model equations were found out which helped in deriving the power flow and torque equations. The four modes of operations were reached at by finding out the equations for the rotor injected e.m.f..

CHAPTER 3

Modelling of DFIG

CHAPTER III: MODELLING OF DFIG

3.1. Vector Control:

There are two ways to divide the complete control strategy of the machine, one is scalar control and the other is vector control. The limited uses of scalar control makes way for vector control. Although it is easy to execute the scalar control strategy, but the inherent coupling effect present gives slow response. This problem is overcome by the vector control, invented in the 1970s. An Induction Motor can be executed like a dc machine with the help of vector control. Vector control is employed to achieve a decoupled control of the active and reactive power.

The basis of the vector control theory is d-q axis theory. Study of the d-q theory is essential for vector control analysis.

3.1.1. d-q axis transformation (reference frame theory):

dq0 or direct-quadrature-zero transformation is a mathematical transformation employed to simplify the analysis of three phase circuits, where three AC quantities are transformed to two DC quantities. The mathematical calculations are performed on the imaginary DC quantities and the AC quantities are again recovered by performing an inverse transformation of the DC quantities. It is similar to Park's transformation, and it also solves the problem of AC parameters varying with time.

Owing to the smooth air-gap in the induction motor, the self-inductance of both the stator and rotor coils are constant, whereas the mutual inductances vary with the rotor displacement with respect to the stator. Therefore the analysis of the induction motor in real time becomes complex due to the varying mutual inductances, as the voltage is not linear. A change of variables is

therefore employed for the stator and rotor parameters to remove the effect of varying mutual inductances. This leads to an imaginary magnetically decoupled two phase machine.

The orthogonally placed balanced windings, called d- and q- windings can be considered as stationary or moving relative to the stator. In the stationary frame of reference, the d^s and q^s axes are fixed on the stator, with either d^s or q^s axis coinciding with the a-phase axis of the stator. In the rotating frame, the rotating d-q axes may be either fixed on the rotor or made to move at the synchronous speed.

3.2.2. Transformation from 3-phase stationary (a, b, c) to 2-phase stationary (d^s, q^s) axes:

$$\begin{bmatrix} V_{qs}^s \\ V_{ds}^s \\ V_{0s}^s \end{bmatrix} = \frac{2}{3} \begin{bmatrix} \cos\theta & \cos(\theta-120) & \cos(\theta+120) \\ sin\theta & \sin(\theta-120) & \sin(\theta+120) \\ 0.5 & 0.5 & 0.5 \end{bmatrix} \begin{bmatrix} V_{as} \\ V_{bs} \\ V_{cs} \end{bmatrix} \quad (3.1)$$

Setting θ=0, aligning q^s-axis with a-axis (In case d^s-axis is aligned with a-axis, replace sine with cosine and vice-versa).

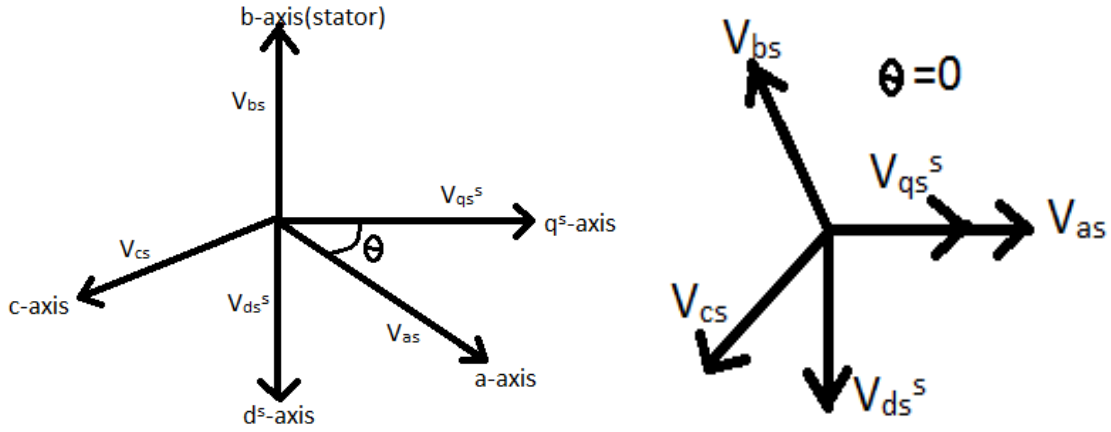

Fig 3.1: Phasor Diagram for abc to dq transformation

$$\begin{bmatrix} V_{qs}^s \\ V_{ds}^s \\ V_{0s}^s \end{bmatrix} = \frac{2}{3} \begin{bmatrix} 1 & -0.5 & -0.5 \\ 0 & 0.866 & -0.866 \\ 0.5 & 0.5 & 0.5 \end{bmatrix} \begin{bmatrix} V_{as} \\ V_{bs} \\ V_{cs} \end{bmatrix} \quad (3.2)$$

3.3.3. Transformation of 2-phase stationary (d^s, q^s) to synchronous 2-phase rotating axes (d, q):

$$V_{qs} = V_{qs}^{s} \cos\theta_e - V_{ds}^{s} \sin\theta_e \tag{3.3}$$

$$V_{ds} = V_{qs}^{s} \sin\theta_e + V_{ds}^{s} \cos\theta_e \tag{3.4}$$

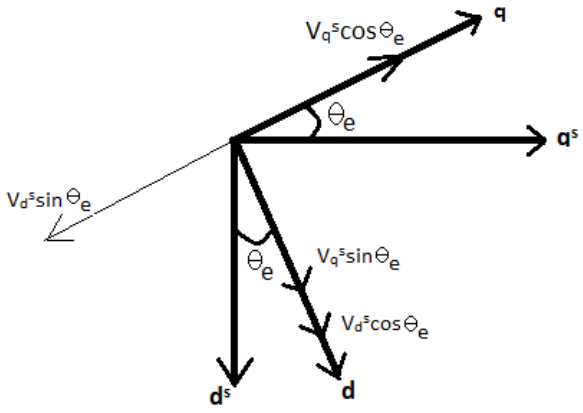

Fig 3.2: Transformation from d^s, q^s to d, q

$$V_{qs}^{s} = V_{qs} \cos\theta_e + V_{ds} \sin\theta_e \tag{3.5}$$

$$V_{ds}^{s} = -V_{qs} \sin\theta_e + V_{ds} \cos\theta_e \tag{3.6}$$

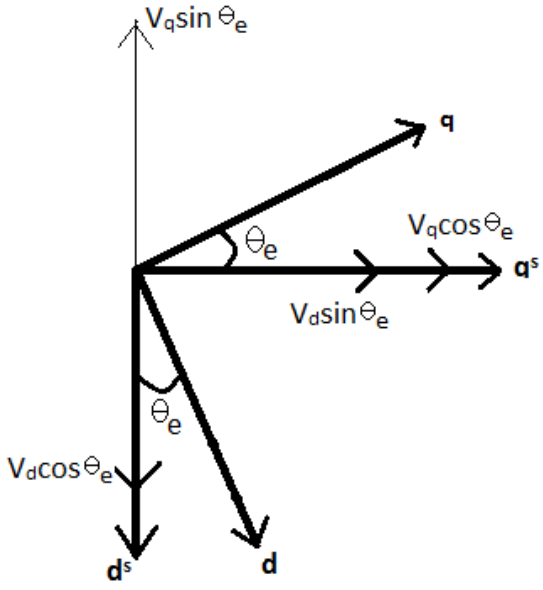

Fig 3.3: Transformation from d, q to d^s, q^s

3.2. Modelling of DFIG (in synchronous (d-q) frame)

Stator circuit equations in d^s-q^s frame:

$$V_{qs}^s = R_s i_{qs}^s + p\psi_{qs}^s \tag{3.7}$$

$$V_{ds}^s = R_s i_{ds}^s + p\psi_{ds}^s \tag{3.8}$$

d-q equivalent circuit (DFIG):

q-axis circuit:

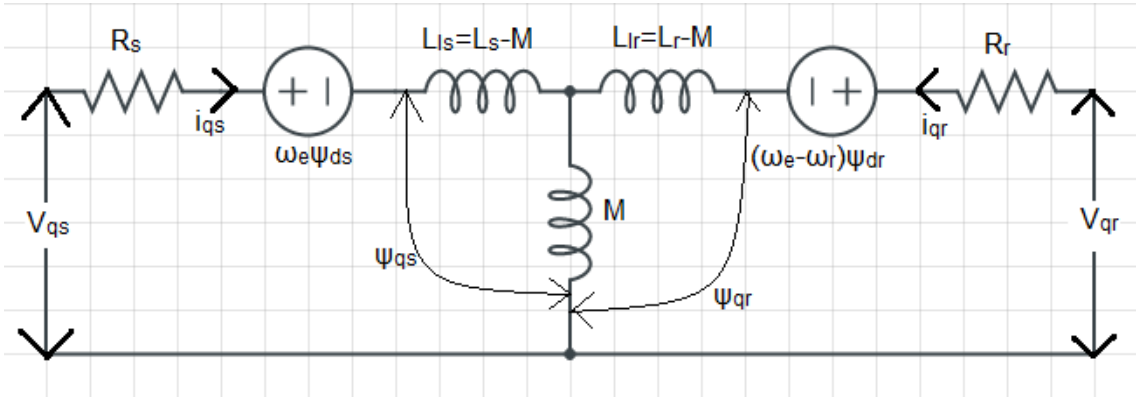

Fig 3.4: q-axis equivalent circuit of DFIG in synchronous (d-q) frame

d-axis circuit:

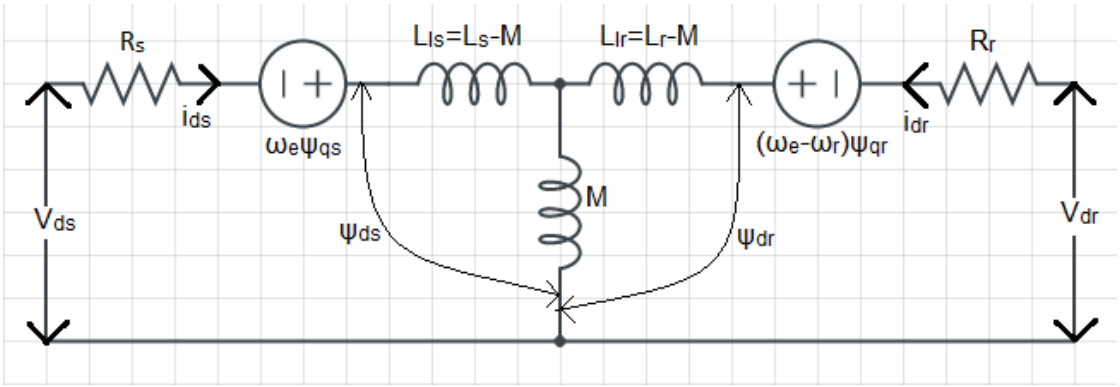

Fig 3.5: d-axis equivalent circuit of DFIG in synchronous (d-q) frame

Stator circuit equations in d-q frame:

$$V_{qs} = R_s i_{qs} + p\psi_{qs} + \omega_e \psi_{ds} \tag{3.9}$$

$$V_{ds} = R_s i_{ds} + p\psi_{ds} - \omega_e \psi_{qs} \tag{3.10}$$

Where, $\omega\psi$ is the back e.m.f .or speed e.m.f. due to rotation of axis.

When the angular speed of the d-q frame i.e. $\omega_e = 0$, the equation changes to stationary form.

Rotor circuit equation in d-q frame:

$$V_{qr} = R_r i_{qr} + p\psi_{qr} + (\omega_e - \omega_r)\psi_{dr} \tag{3.11}$$

$$V_{dr} = R_r i_{dr} + p\psi_{dr} - (\omega_e - \omega_r)\psi_{qr} \tag{3.12}$$

If the rotor is blocked, i.e. $\omega_r = 0$ then,

$$V_{qr} = R_r i_{qr} + p\psi_{qr} + \omega_e \psi_{dr} \tag{3.13}$$

$$V_{dr} = R_r i_{dr} + p\psi_{dr} - \omega_e \psi_{qr} \tag{3.14}$$

Flux Linkage expressions:

$$\psi_{qs} = L_{ls} i_{qs} + L_m (i_{qs} + i_{qr}) = L_s i_{qs} + L_m i_{qr} \tag{3.15}$$

$$\psi_{ds} = L_{ls} i_{ds} + L_m (i_{ds} + i_{dr}) = L_s i_{ds} + L_m i_{dr} \tag{3.16}$$

$$\psi_{qr} = L_{lr} i_{qr} + L_m (i_{qs} + i_{qr}) = L_r i_{qr} + L_m i_{qs} \tag{3.17}$$

$$\psi_{dr} = L_{lr} i_{dr} + L_m (i_{ds} + i_{dr}) = L_r i_{dr} + L_m i_{ds} \tag{3.18}$$

Where $L_s = L_m + L_{ls}$ and $L_r = L_m + L_{lr}$

$$\psi_{qm} = L_m (i_{qs} + i_{qr}) \tag{3.19}$$

$$\psi_{dm} = L_m (i_{ds} + i_{dr}) \tag{3.20}$$

Equations (3.7) to (3.20) describe the overall electrical modeling of the DFIG. The equation below explains the mechanical aspect.

3.3. Conclusion

The vector control theory was studied which helped in transforming the three phase quantities to two phase so that decoupled control could be achieved. The vector control was achieved using d-q transformation of quantities which lead to the equivalent circuit model for the d and q axis in the synchronous frame of reference. The stator, rotor and flux linkage expressions were then found out once the equivalent circuit had been achieved.

CHAPTER 4

Synchronised Model of DFIG

CHAPTER IV: SYNCHRONISED MODEL OF DFIG

4.1. Modelling of the DFIG Stator:

The accuracy is not affected much if we neglect the stator transients, after the transients have damped out. So $p\psi_{qs} = 0$ and $p\psi_{ds} = 0$. Taking stator in generator convention and rotor in motor convention, we have:

$$u_{d1} = -r_1 i_{d1} - \psi_{q1}\omega_1 \tag{4.1}$$

$$u_{q1} = -r_1 i_{q1} - \psi_{d1}\omega_1 \tag{4.2}$$

Where $\omega_1 = \omega_e$

$$u_{d2} = -r_2 i_{d2} - \psi_{q2}\omega_2 + p\psi_{d2} \tag{4.3}$$

$$u_{q2} = -r_2 i_{q2} - \psi_{d2}\omega_2 + p\psi_{q2} \tag{4.4}$$

Where $\omega_2 = \omega_r - \omega_e$

The corresponding flux linkage expressions are,

$$\psi_{d1} = -L_1 i_{d1} - L_m i_{d2} \tag{4.5}$$

$$\psi_{q1} = -L_1 i_{q1} + L_m i_{q2} \tag{4.6}$$

$$\psi_{d2} = L_2 i_{d2} - L_m i_{d1} \tag{4.7}$$

$$\psi_{q2} = L_2 i_{q2} - L_m i_{q1} \tag{4.8}$$

Aligning d-axis with the rotor flux vector, we have

$$\psi_2 = \psi_{d2} \Rightarrow \psi_{q2} = 0$$

Rotor currents can be expressed in terms of stator currents as follows:

$$i_{d2} = \frac{\psi_2 + L_m i_{d1}}{L_2} \tag{4.9}$$

$$i_{q2} = \frac{L_m}{L_2 i_{q1}} \tag{4.10}$$

In order to eliminate the rotor variables in the stator equations, we define:

$$E'_q = \omega_1 \frac{L_m}{L_2} \psi_2 \tag{4.11}$$

Where E'_q is the equivalent e.m.f. behind the internal transient reactance, generated by the rotor linkage ψ_2

$$X'_1 = \sigma \omega_1 L_1 \tag{4.12}$$

$$\sigma = \frac{L_1 L_2 - L_m^2}{L_1 L_2} \tag{4.13}$$

Where X'_1 is the transient reactance of the stator.

$$u_{d1} = -r_1 i_{d1} + X'_1 i_{q1} \tag{4.14}$$

$$u_{q1} = -r_1 i_{q1} - X'_1 i_{d1} + E'_q \tag{4.15}$$

From (4.14) and (4.15), making r_1=0, $u_{d1} = U_1 \sin\delta$ and $u_{q1} = U_1 \cos\delta$,

$$i_{d1} = \frac{E'_q - U_1 \cos\delta}{X'_1} \tag{4.16}$$

$$i_{q1} = \frac{U_1 \sin\delta}{X'_1} \tag{4.17}$$

4.2. Stator Active and Reactive Powers:

$$P_1 = U_1 I_1 \cos\phi = \frac{E'_q U_1 \sin\delta}{X'_1} \tag{4.18}$$

$$Q_1 = U_1 I_1 \sin\phi = \frac{E'_q U_1 \cos\delta}{X'_1} - \frac{U_1^2}{X'_1} \tag{4.19}$$

The stator active power P depends mainly on the power angle (which can be controlled by the rotor converter) whereas the stator reactive power Q depends on the voltage magnitude of E'_q.

The stator active and reactive powers can be controlled by controlling the phase and magnitude of E'_q.

Also,

$$P_1 = u_{d1} i_{d1} + u_{q1} i_{q1} \tag{4.20}$$

$$Q_1 = u_{q1} i_{d1} - u_{d1} i_{q1} \tag{4.21}$$

4.3. Modelling of the DFIG Rotor:

By using (4.3), (4.4), (4.9) and (4.10) rotor voltages can be expressed as:

$$u_{d2} = r_2 \frac{\psi_2}{L_2} + r_2 \frac{L_m}{L_2} i_{d1} + p\psi_2 \tag{4.22}$$

$$u_{q2} = r_2 \frac{L_m}{L_2} i_{q1} + \psi_2 \omega_2 \tag{4.23}$$

$$\Rightarrow U_2 = r_2 \frac{L_m}{L_2} I_1 + (\frac{r_2 + pL_2 + \omega_2 L_2}{\omega_1 L_m}) E'_q \tag{4.24}$$

Replacing $I_1 = \frac{E'_q - U_1}{X'_1}$ in the above equation, we have

$$U_2 = \left(\frac{r_2 L_m}{L_2 X'_1} + \frac{r_2 + pL_2 + \omega_2 L_2}{\omega_1 L_m} \right) E'_q - \frac{r_2 L_m}{L_2 X'_1} U_1 \tag{4.25}$$

The above equation describes the relationship between the stator voltage U_1, rotor voltage U_2, internal transient e.m.f. vector E'_q. E'_q can be controlled by U_2 (keeping grid voltage fixed).

4.4. Conclusion

This chapter described further modelling of the DFIG using the parameters generated in the previous chapter. Using certain assumptions such as neglecting stator transients, the simplified form of modelling was achieved for the stator and the rotor in the synchronous frame of reference. The transient reactance of the stator and the equivalent e.m.f. behind it was used to find out independent equations for the rotor and stator voltage and currents, which can then be used for finding out the active and reactive powers leading to decoupled control of the same.

CHAPTER 5

Simulation

CHAPTER V: SIMULATION

5.1. Pitch Control using MATLAB

An equation used to model $C_p(\lambda,\beta)$ is given as:

$$C_p(\lambda,\beta)=c_1\left(\frac{c_2}{\lambda}-c_3\beta-c_4\right)e^{\frac{c_5}{\lambda_i}}+c_6\lambda \tag{5.1}$$

With

$$\frac{1}{\lambda_i}=\frac{1}{\lambda+0.08\beta}-\frac{0.035}{\beta^3+1} \tag{5.2}$$

Where

$c_1 = 0.5176$, $c_2 = 116$, $c_3 = 0.4$, $c_4 = 5$, $c_5 = 21$, $c_6 = 0.0068$.

The Cp-λ characteristics, for various values of the pitch angle β, are plotted below.

RESULT:

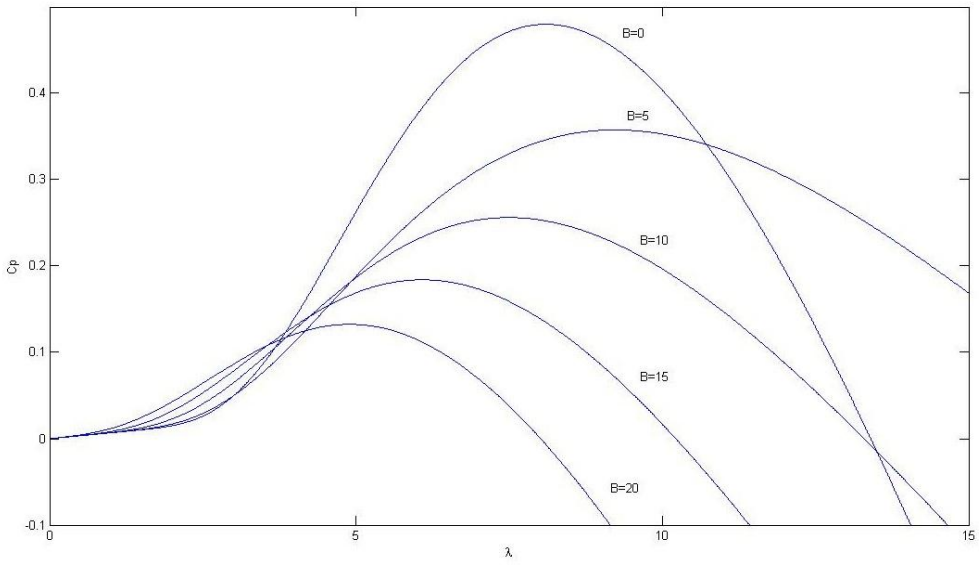

Figure 5.1: C_p ~ TSR Characteristics for different pitch angles

The maximum value of C_p (C_{pmax} = 0.48) is achieved for β = 0 degree at λ = 8.1

5.2. Power-Speed Characteristics Analysis using MATLAB

$$P_m = 0.5 C_p A \rho V_\infty^3 \tag{5.3}$$

$$C_p(\lambda, \beta) = c_1 \left(\frac{c_2}{\lambda} - c_3\beta - c_4\right) e^{\frac{c_5}{\lambda_i}} + c_6\lambda$$

RESULT:

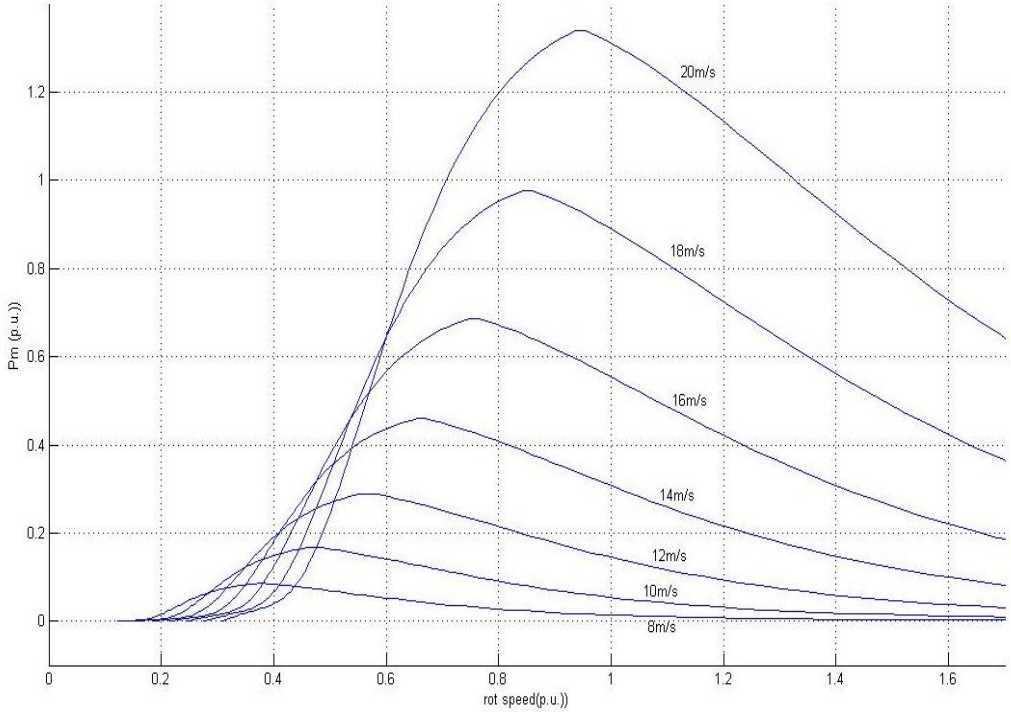

Figure 5.2: Power ~ Rot Speed (p.u.) for blade angle = 0 deg for varying wind speed

5.3. TORQUE-SLIP CHARACTERISTICS ANALYSIS USING MATLAB

5.3.1. Torque-slip characteristic when angle of E_j is 0, $|E_j|$ changing from 0 to +0.05 pu:

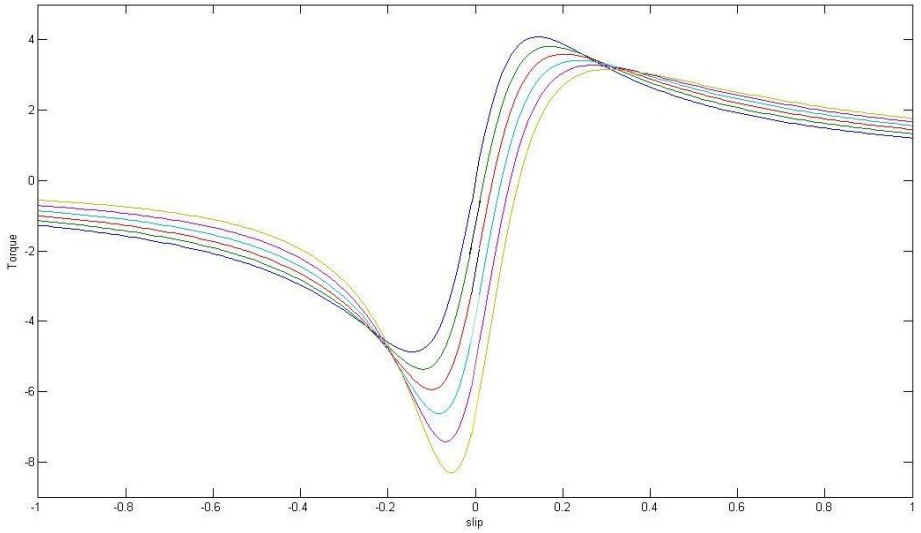

Fig 5.3: Torque slip characteristics for magnitude of E_j varying.

5.3.2. Torque-slip characteristic when the $|E_j|$ is 0.05 pu. Angle of E_j changing from -180 to +180:

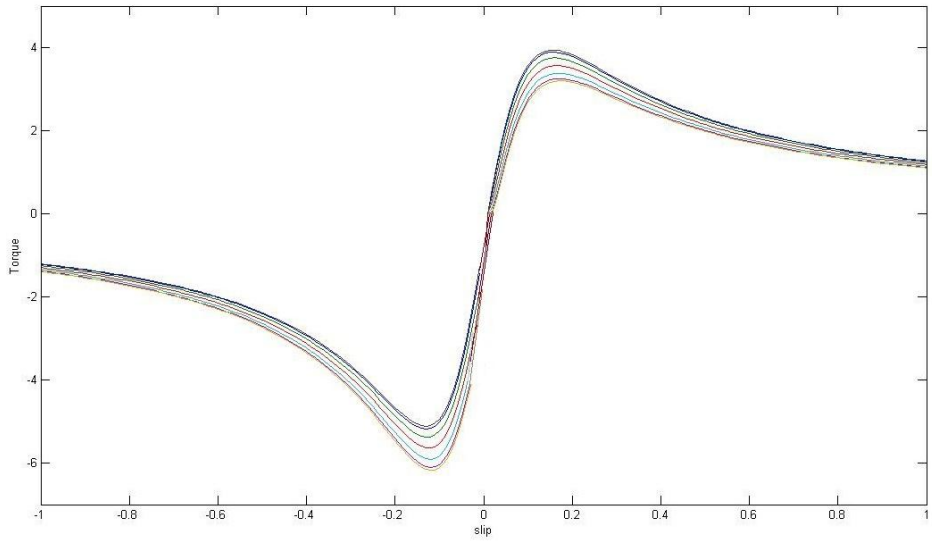

Fig 5.4: Torque slip characteristics for angle of E_j varying.

5.4. STUDY OF DFIG WIND FARM (AVERAGE MODEL)

In this type of model the IGBT Voltage-sourced converters (VSC) are represented by equivalent voltage sources generating the AC voltage averaged over one cycle of the switching frequency. A 9 MW wind farm whose parameter detail are given in Appendix I is simulated using MATLAB/SIMULINK environment.

The performance of the system is studied under grid voltage fluctuations. The voltage variations are made by decreasing and increasing the grid voltage for simulation purpose. For the performance analysis of the system, the effects due to wind speed and supply frequency variation are also taken into account. The analysis is also done by changing the demand of reactive power of machine.

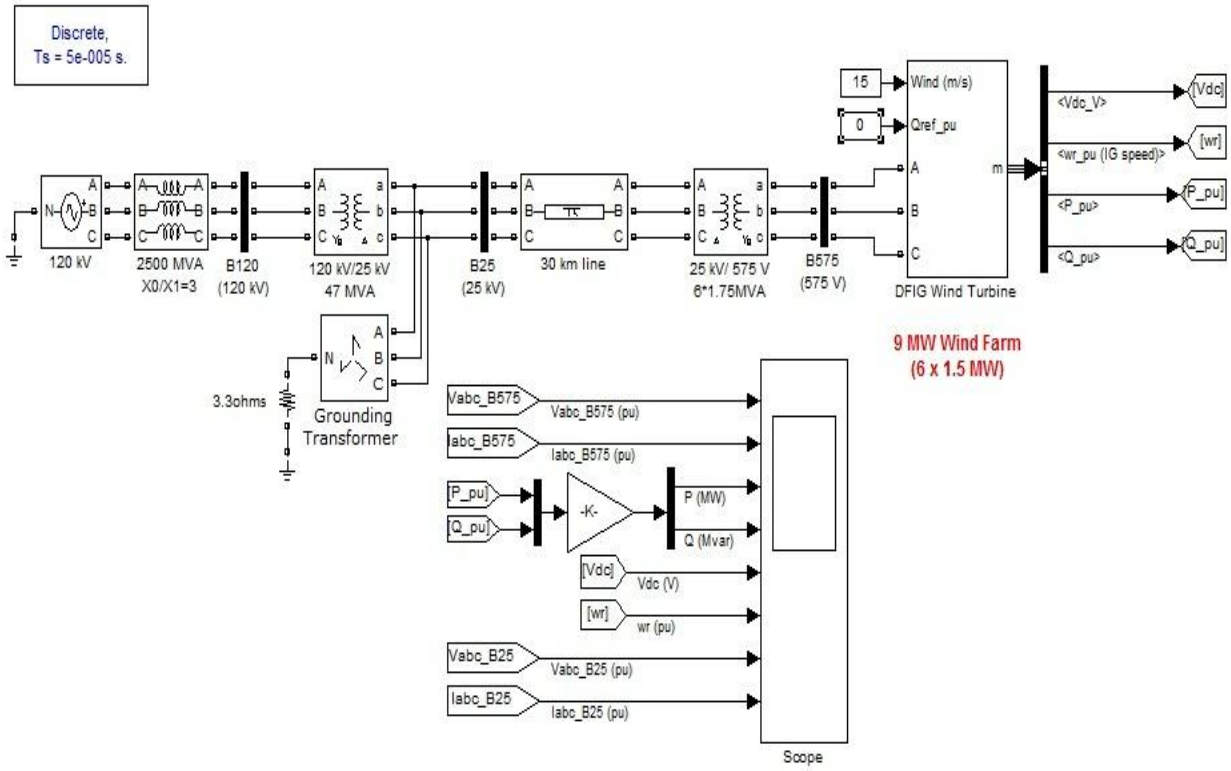

Fig 5.5: Matlab/Simulink DFIG Average Model

5.4.1. Simulation under balanced grid:

The characteristic waveforms of DFIG under balanced grid conditions are shown in Fig 4.6. It is observed that the active and reactive powers supplied by the utility grid are decoupled and dc link voltage is maintained constant due to the control strategy made in the grid side converter.

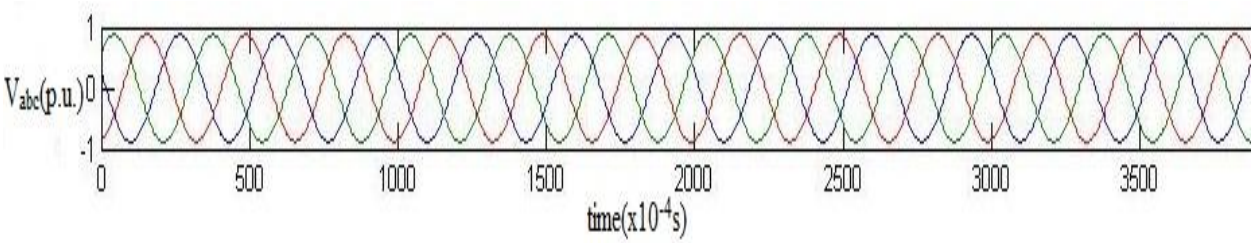

Fig 5.6a: Stator Voltage

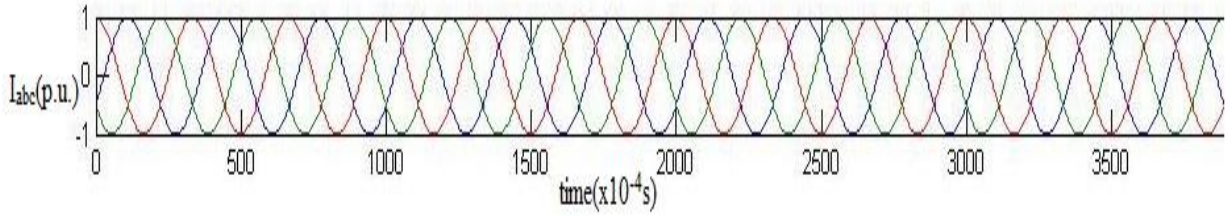

Fig 5.6b: Stator Current

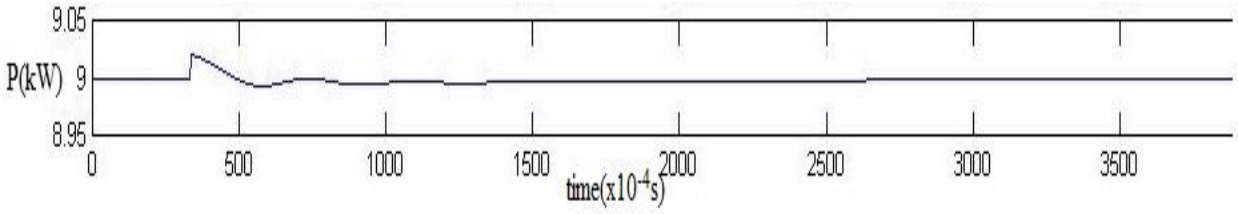

Fig 5.6c: Active Power

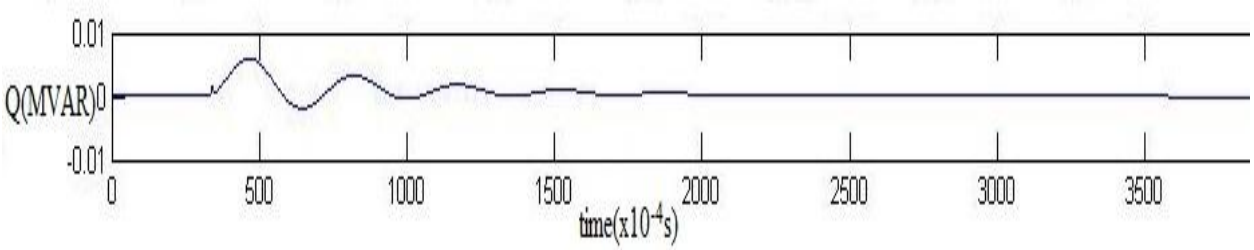

Fig 5.6d: Reactive Power

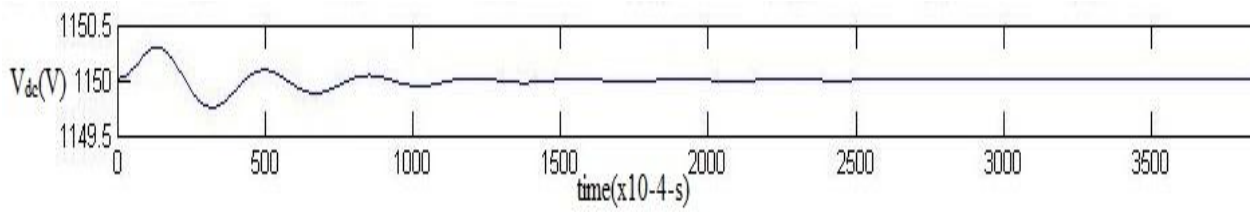

Fig 5.6e: DC-Link Voltage

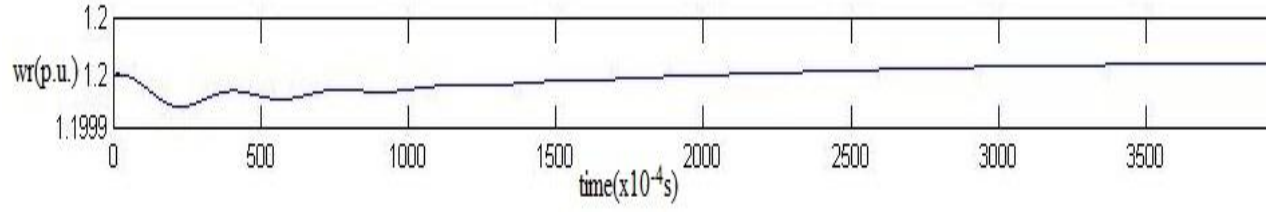

Fig 5.6f: Rotor Speed

5.4.2. Simulation under Voltage sag:

The simulation results under the voltage sag are shown in Fig.4.7. A voltage drop of 0.5 p.u. is programmed for 0.1 s starting at 0.03s. The system produces active power of 9 MW which corresponds to maximum mechanical turbine output minus electrical losses in generator. When the grid voltage decreases suddenly from its rated value, the stator current as well as rotor current increases and the active power P rises for a very brief time and then drops, and finally settles at the rated value. The reference reactive power is set at 0MVAr but during the sag it suddenly

increases finally settling to 0kVAr as per the control strategy made in the rotor side converter. The dc link voltage oscillates from its set value of 1150V and finally settles at its set value and the rotor speed is also maintained constant to its rated (1.2 p.u.) value while the wind speed is kept constant at 15m/s.

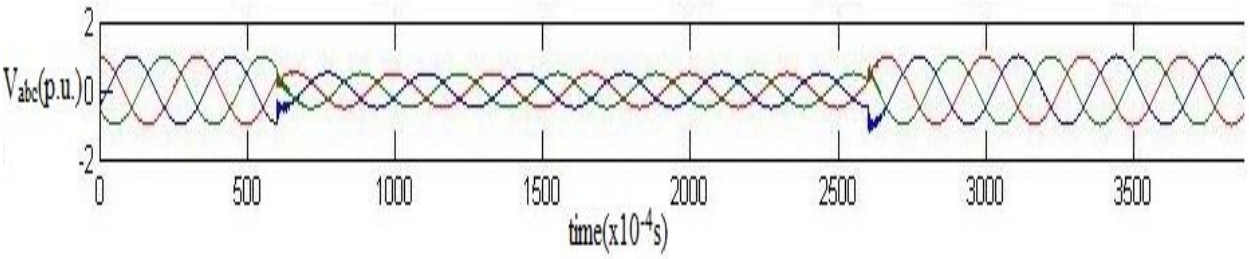

Fig 5.7a: Stator Voltage

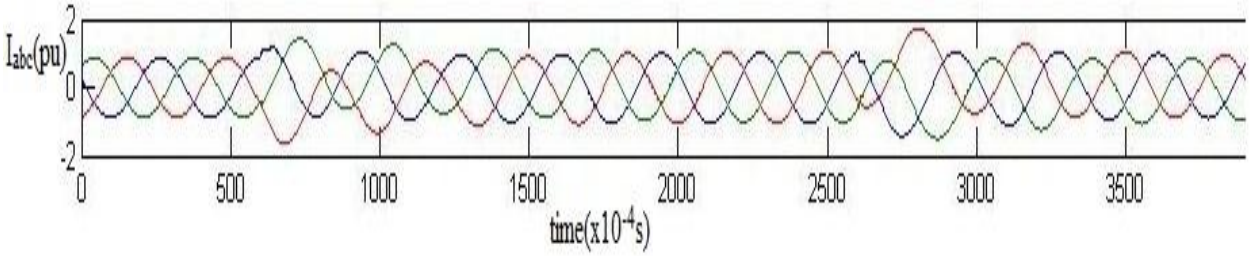

Fig 5.7b: Stator Current

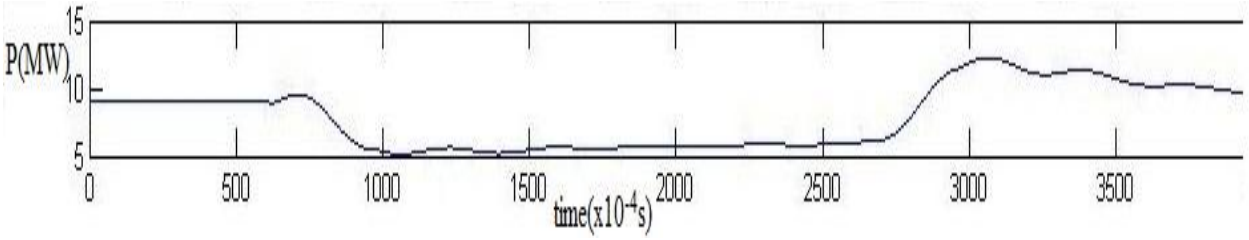

Fig 5.7c: Active Power

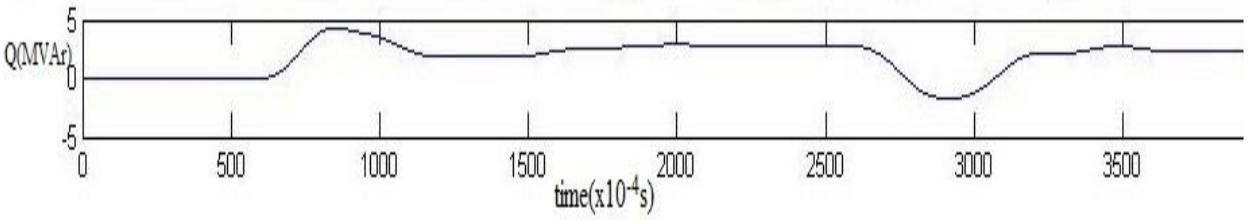

Fig 5.7d: Reactive Power

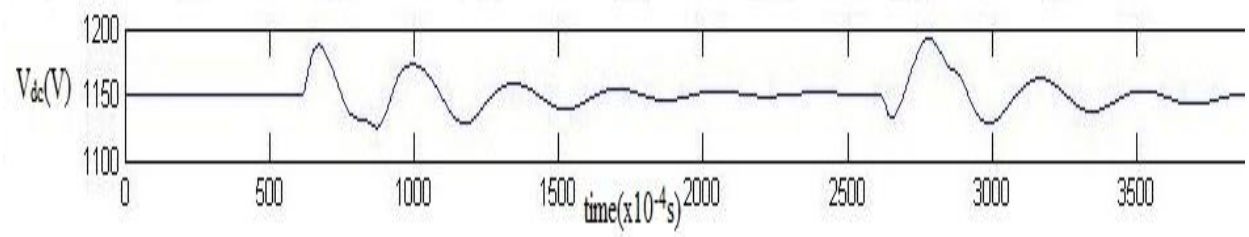

Fig 5.7e: DC-Link Voltage

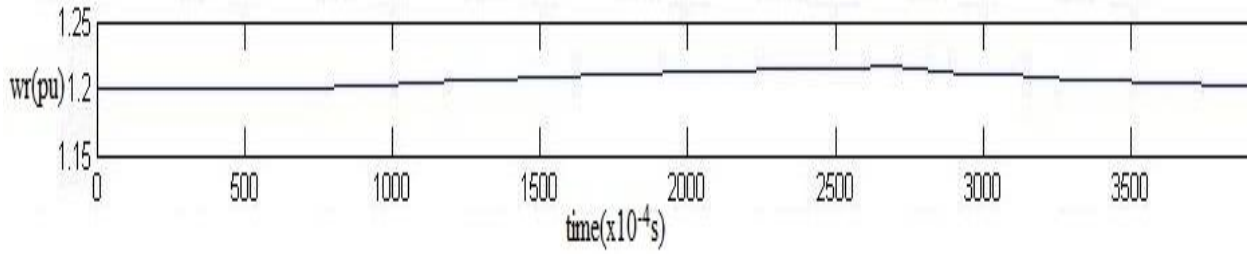

Fig 5.7f: Rotor Speed

5.4.3. Simulation under Voltage Swell:

Simulation results under voltage swell is shown in Fig 4.8. When the grid voltage increases up to 150% of its rated value, the stator current as well as rotor current decreases. The active power rises for a brief time and then settles at the rated value and the reactive power decreases suddenly and then settles at 0kVAr. The DC-link voltage oscillates before settling at the rated value. The rotor speed and wind speed are maintained constant.

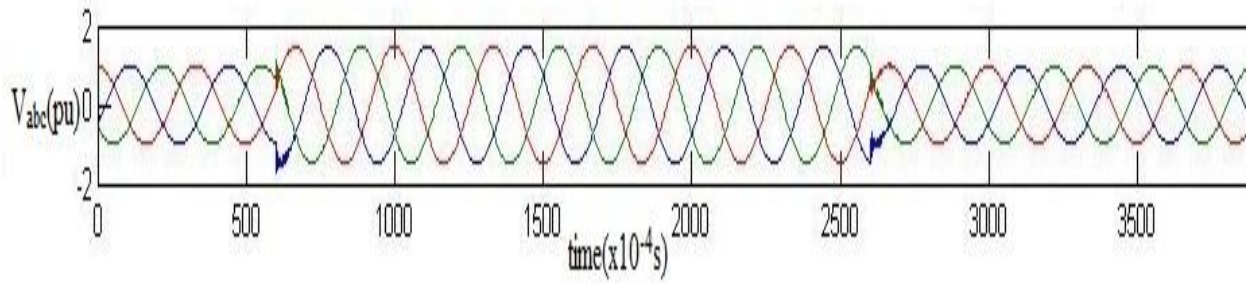

Fig 5.8a: Stator Voltage

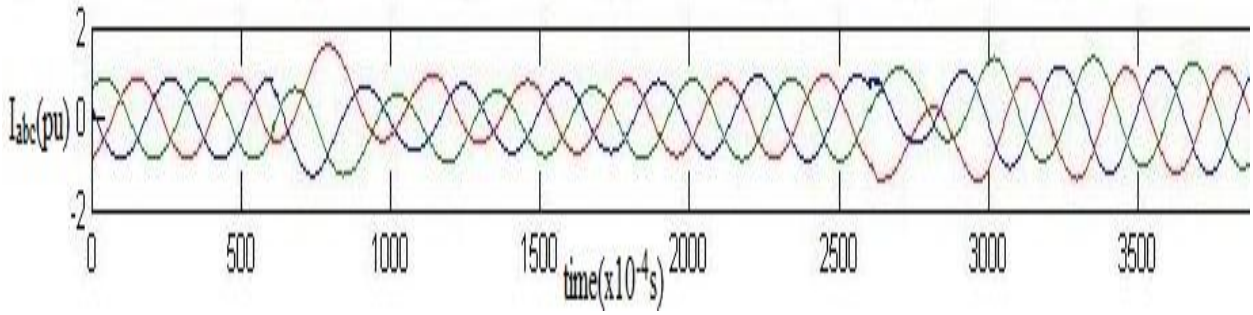

Fig 5.8b: Stator Current

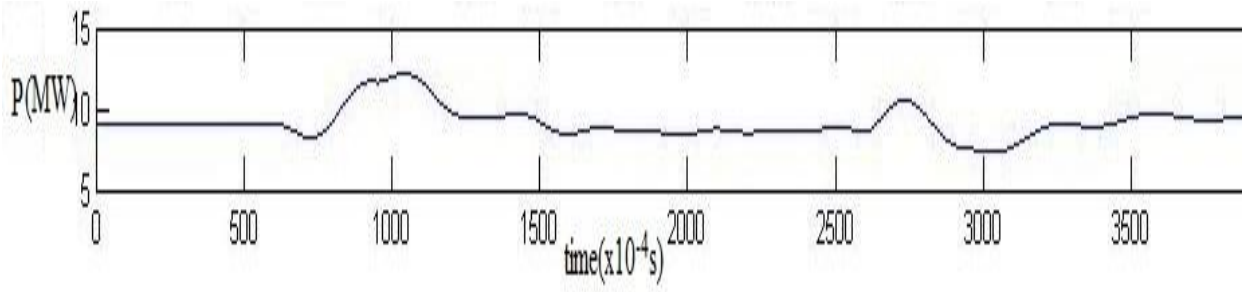

Fig 5.8c: Active Power

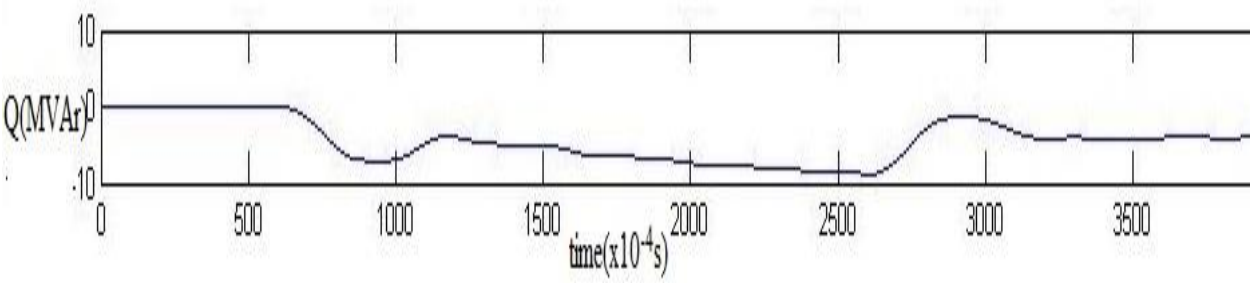

Fig 5.8d: Reactive Power

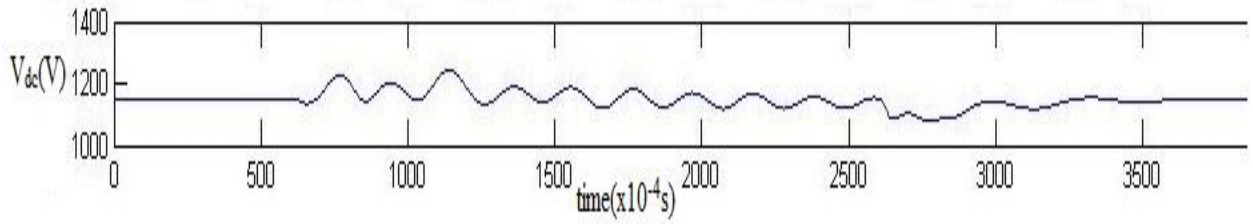

Fig 5.8e: DC-Link Voltage

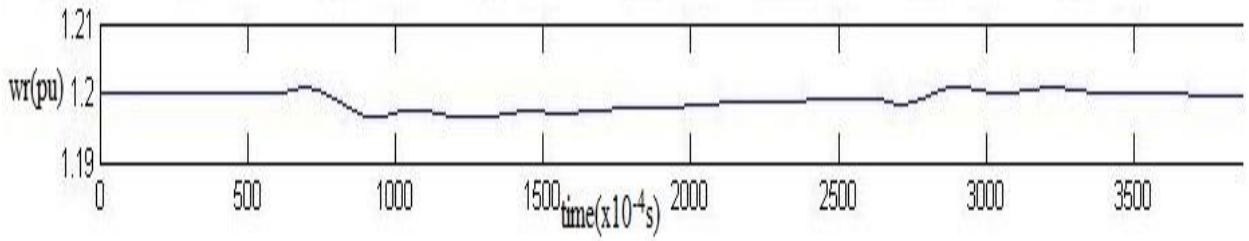

Fig 5.8f: Rotor Speed

5.4.4. Simulation under change in reactive power demand:

The Fig.4.8 shows the variation of the parameters during voltage swell when the reactive power demand is set to 1p.u. instead of 0 p.u.

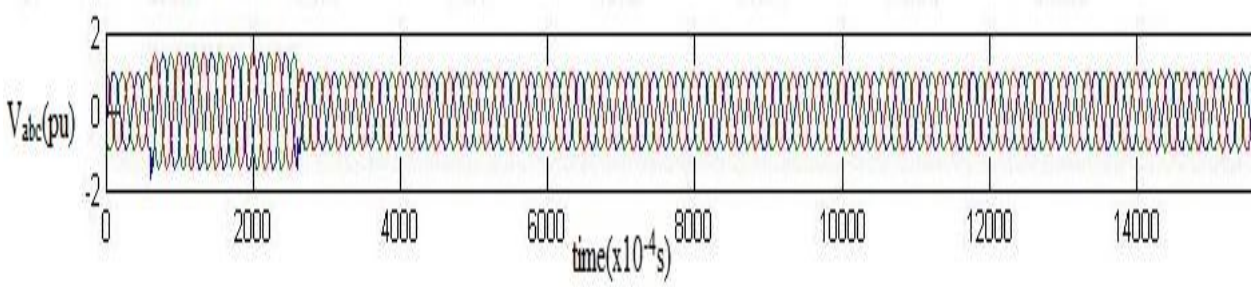

Fig 5.9a: Stator Voltage

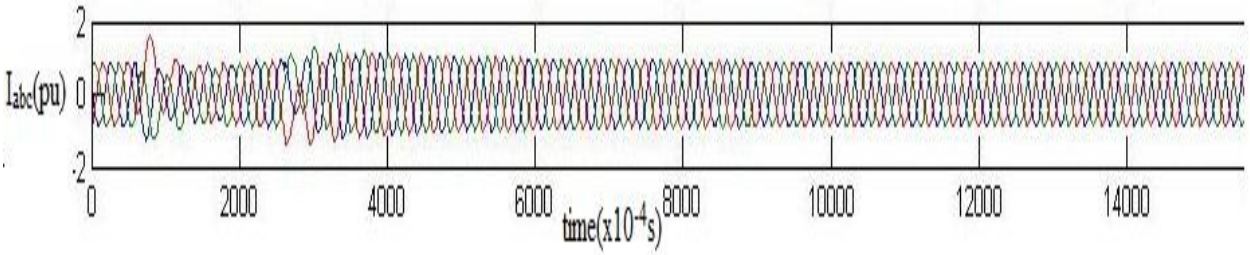

Fig 5.9b: Stator Current

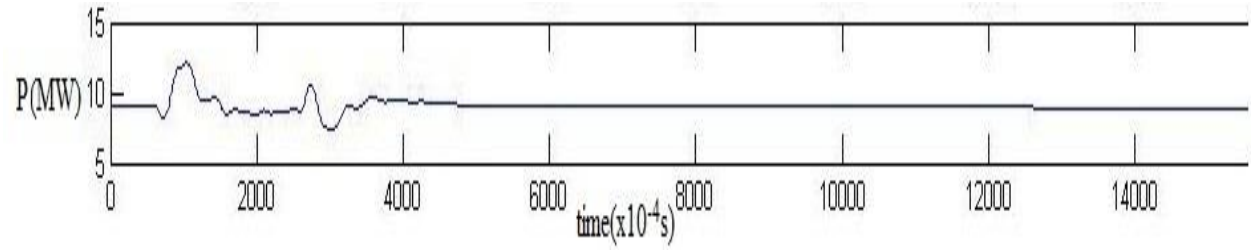

Fig 5.9c: Active Power

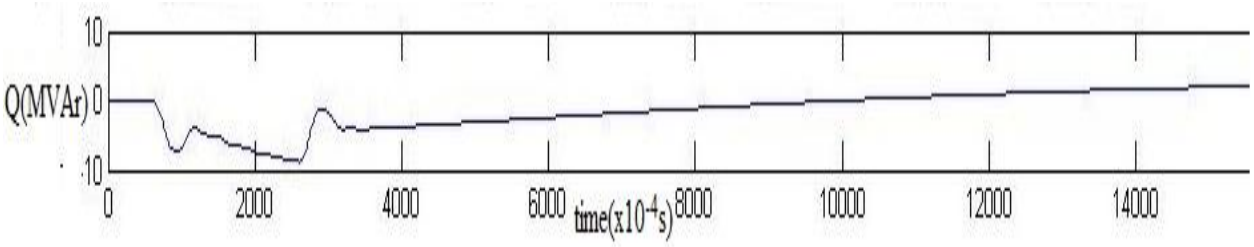

Fig 5.9d: Reactive Power

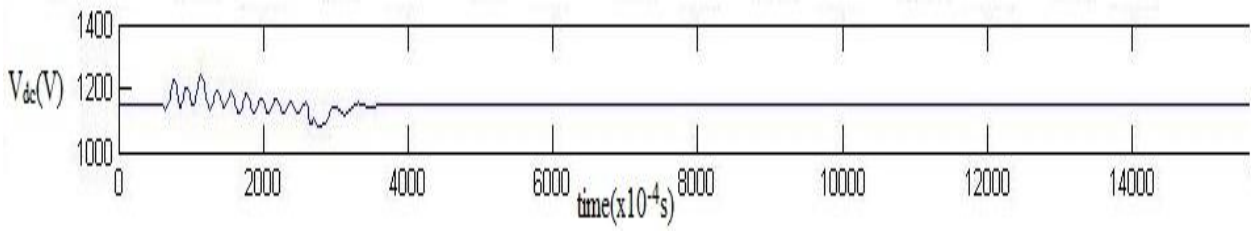

Fig 5.9e: DC-Link Voltage

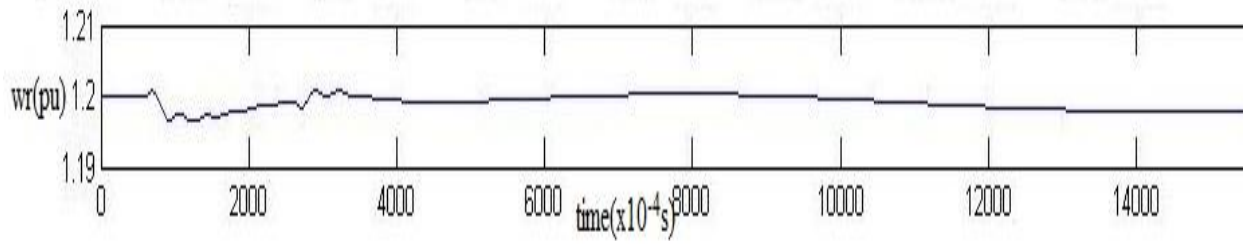

Fig 5.9f: Rotor Speed

5.4.5. Simulation under wind speed variation:

When the wind speed changes suddenly from 15m/s to 16m/s the rotor speed increases gradually and then after a brief while it settles to its rated value of 1.2p.u.as per the control strategy made in the rotor side converter. The voltage and current magnitude remain the same as 4.6. A ramp with a rising slew rate limited to four is used to generate the change in the wind speed between

the interval 0.01 to 0.13 seconds. The rotor speed increases for a while and then falls to the rated value because the control system employs a torque controller in order to maintain the rotor speed at 1.2 p.u. As the active power increases the pitch angle also increases from initial 8.7 to 11.5 degrees, to limit the mechanical power output.

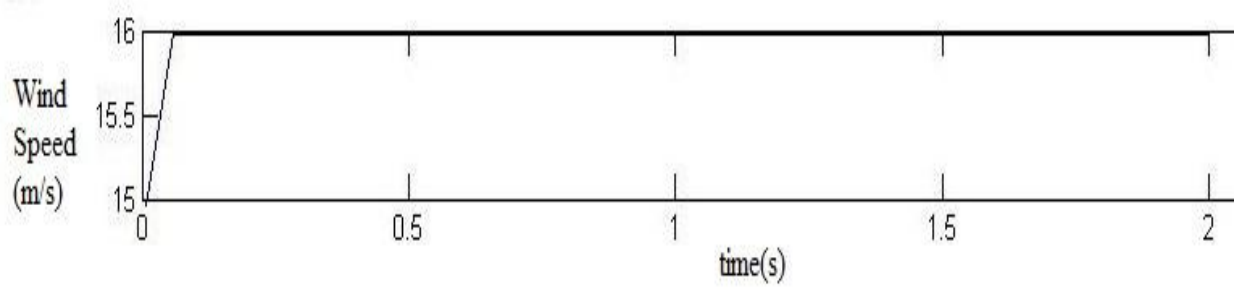

Fig 5.10a: Wind Speed

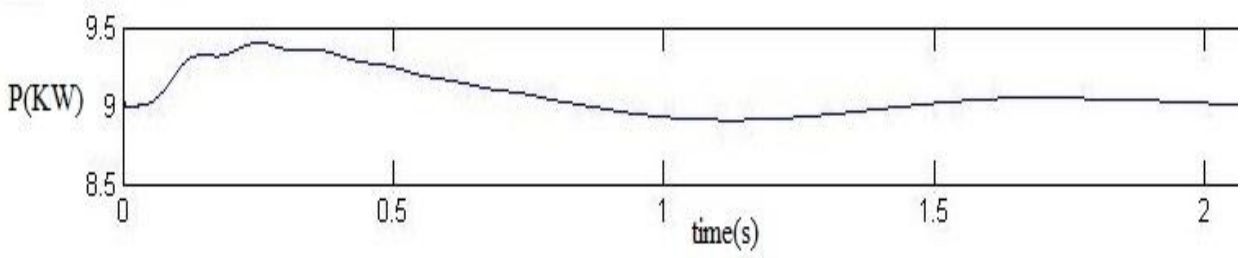

Fig 5.10b: Active Power

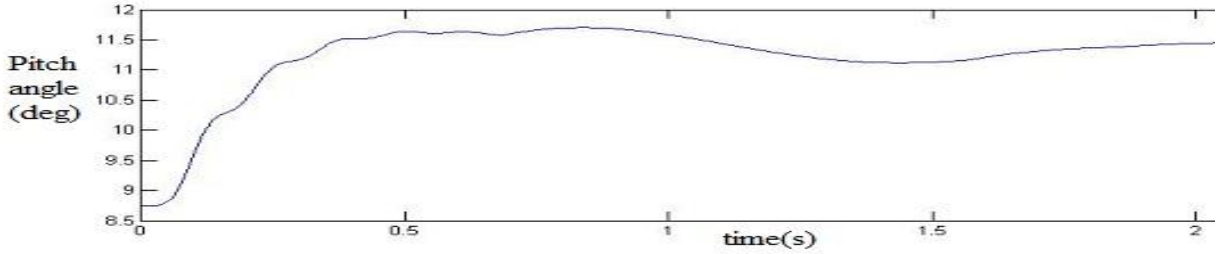

Fig 5.10c: Pitch Angle

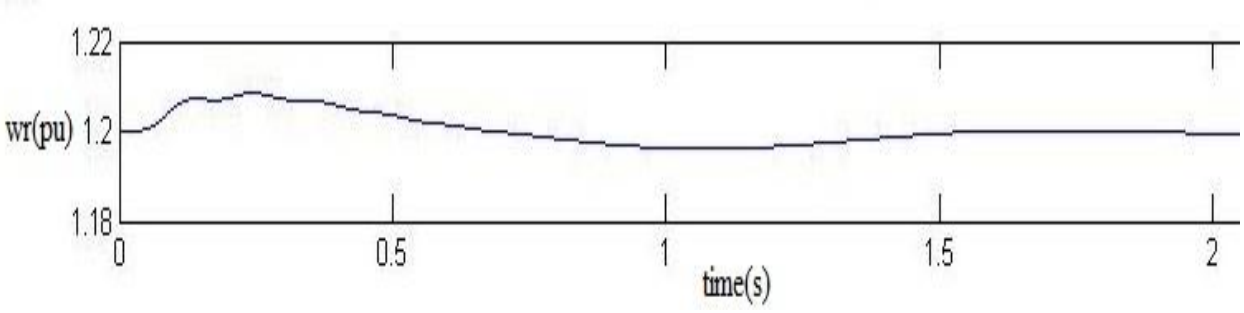

Fig 5.10d: Rotor Speed

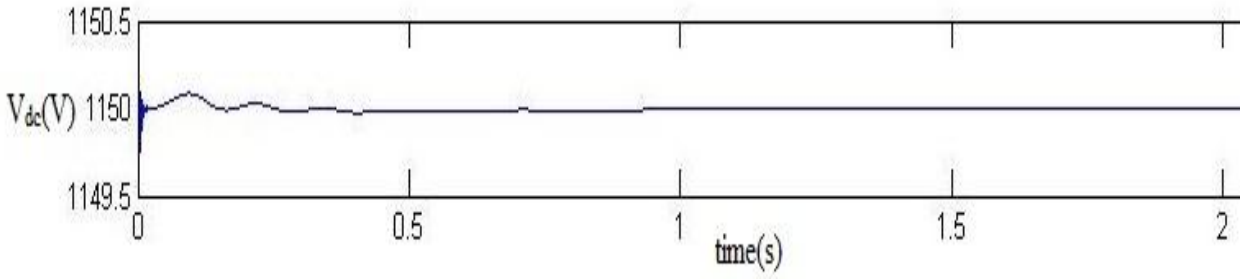

Fig 5.10e: DC-link Voltage

5.5. Conclusion

This chapter covers the complete simulation of the characteristics curves and the average model of the wind farm. In case of the pitch control the maximum value of C_p was achieved for $\beta = 0$ degree at $\lambda = 8.1$. The power speed characteristics were also found out for various wind speeds and are in accordance with the theory established. Decoupled control was achieved by changing either the magnitude or the angle of the rotor injected e.m.f. and the variation of the torque for the same was shown with respect to the speed. Lastly a wind farm model employing pitch control and torque controller was studied under fluctuations of the wind speed and grid voltage.

CHAPTER 6

Conclusion and Future Work

6.1. Conclusion

The theory of the wind turbine was analyzed in detail leading to the modelling in the synchronous frame of reference employing a doubly fed induction generator. The pitch control characteristics were found out and the power speed characteristics were derived for various wind speeds. Also the rotor injected e.m.f. showed that the active and reactive power could be controlled by changing the magnitude and angle of the rotor injected e.m.f. respectively. The wind farm average model was studied under various voltage fluctuations and is in accordance with the operating principles of the doubly fed induction generator, the DC Link voltage remained constant despite voltage sag or swell and other fluctuations, also the active and reactive power, rotor speed finally settle at the rated value after the transient is over. Pitch control employed checked the mechanical power output during increase in the wind speed as studied earlier.

6.2. Future Work:

The wind farm studied operates at grid frequency of 60Hz. The model can be modified to suit the needs of the particular place such as 50Hz for India and the rating of the DFIG can be modified which includes complete modification of the various stator, rotor and turbine parameters. Also the voltage source converters have been replaced with constant voltage sources for less complications, the detailed model can be reached at by using IGBT based voltage source converters. Also methods for further decoupling of active and reactive power can be found out by further research work to increase the efficiency.

REFERENCES

[1] Hector A. Pulgar-Painemal, Peter W. Sauer, "Doubly Fed Induction Machine in Wind Power Generation," University of Illinois, US, 2009.

[2] John Fletcher and Jin Yang, "Introduction to Doubly-Fed Induction Generator for Wind Power Applications," University of Strathclyde, Glasgow, UK, 2009.

[3] S.N.Bhadra, D.Kashta, S.Banerjee, "Wind Electrical Systems," 3rd Edition, Oxford University Press, India, 2008.

[4] Olimpo Anaya Lara, Nick Jenkins, "Wind Energy Generation," 1st Edition, John Wiley and Sons, UK, 2009.

[5] R. Scherer, "Blade design aspect," Renewable Energy, vol.16, pp.1272-1277, 1999.

[6] Jasmin Martinez, "Modelling and Control of Wind Turbines," Imperial College London, UK, 2007.

[7] Z. Saad-Saoud, N. Jenkins, "Simple Wind Farm Dynamic Model," IEE Proceedings: Generation, Transmission and Distribution, vol.142, no.5, pp.545-548, 1995.

[8] H.A. Pulgar-Painemal, P.W. Sauer, "Dynamic Modeling of Wind Power Generation," North American Power Symposium, Mississippi, 2009.

[9] A. Praveen Varma, K. Bala Chakri, "Study of Grid Connected Induction Generator for Wind Power Applications," Electrical Engineering, NIT Rourkela, 2012.

[10] Satish Choudhury, "Performance Analysis of Doubly-fed Induction Generator in Wind Energy Conversion System," Electrical Engineering, NIT Rourkela, 2011.

APPENDIX

DFIG- Rating and Specifications

VA Rating	10MVA
Rated Power	9MW
Grid Voltage	120kV
Grid Frequency	60Hz
Stator Resistance	0.02 p.u.
Stator Reactance	0.18 p.u.
Rotor resistance(referred to stator)	0.015 p.u.
Rotor reactance(referred to stator)	0.15 p.u.
Magnetizing Inductance	3 p.u.
Rated Speed(p.u. of synchronous speed)	1.2
DC Link Voltage	1150V
Poles	6
DC Link Capacitor	11mF
Pitch Angle	9 deg
Nominal Stator Voltage(rms)	570V